МІНІСТЕРСТВО ОСВІТИ ТА НАУКИ УКРАЇНИ
НАЦІОНАЛЬНИЙ АВІАЦІЙНИЙ УНІВЕРСИТЕТ
КАФЕДРА КОНСТРУКЦІЇ ЛІТАЛЬНИХ АПАРАТІВ

ДОПУСТИТИ ДО ЗАХИСТУ
Завідувач кафедри, д.т.н., проф.
_____ Сергій ІГНАТОВИЧ
«____» _____ 2022 р.

ДИПЛОМНА РОБОТА
ВИПУСКНИКА ОСВІТНЬОГО СТУПЕНЯ «МАГІСТР»
ЗІ СПЕЦІАЛЬНОСТІ:
«АВІАЦІЙНА ТА РАКЕТНО-КОСМІЧНА ТЕХНІКА»

Тема: «Числова симуляція лазерового шокового мотузку з'єднальника з гелікоптером з титаном»

Виконавець: _____ **Цзяюй ХАО**

Керівник: к.т.н., доц. _____ **Вадим ЗАКІЄВ**

Консультанти з окремих розділів пояснювальної записки:
охорона праці:
к.біол.н., доц. _____ **Катериніа КАЖАН**

охорона навколишнього середовища:
к.г.н., доц. _____ **Леся ПАВЛЮХ**

Нормоконтролер: к.т.н, доц. _____ **Володимир КРАСНОПОЛЬСКИЙ**

Київ 2022

MINISTRY OF EDUCATION AND SCIENCE OF UKRAINE
NATIONAL AVIATION UNIVERSITY
DEPARTMENT OF AIRCRAFT DESIGN

PERMISSION TO DEFEND
Head of the department,
Professor, Dr. of Sc.
_____ Serhiy IGNATOVYCH
«___» _____ 2022

MASTER DEGREE THESIS
ON SPECIALITY
"AVIATION AND AEROSPACE TECHNOLOGIES "

Topic: "Numerical simulation of laser shock peening of titanium helicopter hub connector"

Fulfilled by: _____ **Jiayu HAO**

Supervisor:
PhD, associate professor _____ **Vadim ZAKIEV**

Labor protection advisor:
PhD, associate professor _____ **Catarina KAJAN**
Environmental protection adviser:
Dr. Sc., associate professor _____ **Lesya PAVLYUKH**

Standards inspector
PhD, associate professor _____ **Volodymyr KRASNOPOLSKY**

Kyiv 2022

НАЦІОНАЛЬНИЙ АВІАЦІЙНИЙ УНІВЕРСИТЕТ

Аерокосмічний факультет
Кафедра конструкції літальних апаратів
Освітній ступінь «Магістр»
Спеціальність 134 «Авіаційна та ракетно-космічна техніка»
Освітньо-професійна програма «Обладнання повітряних суден»

ЗАТВЕРДЖУЮ
Завідувач кафедри, д.т.н, проф.
_____ Сергій ІГНАТОВИЧ
«_____» _____ 2022 р.

ЗАВДАННЯ

на виконання дипломної роботи студента

ЦЗЯЮЙ ХАО

1. Тема роботи: «Числова симуляція лазерового шокового мотузку з'єднальника з гелікоптером з титаном», затверджена наказом ректора від 05 жовтня 2022 року №1861/ст.
2. Термін виконання роботи: з 06 жовтня 2022 р. по 10 листопад 2022 р.
3. Вихідні дані до роботи: Конституючі параметри моделі Johnson-Cook для матеріалу ститанової легенди ТВ6.
4. Зміст пояснювальної записки: Аналіз застосування лазерового шоку в авіаційній індустрії, досліджується новий багатопunktовий алгоритм, аналізує оптимальні процесові параметри однієї точки ударної діри стіни і обмеження діри, отримає найкращу швидкість перекриття багатопunktів.
5. Перелік обов’язкового графічного (ілюстративного) матеріалу: Лазерний діапазон енергії, механічні параметри властивості ТБ6 титану.

6. Календарний план-графік:

№	Завдання	Термін виконання	Відмітка про виконання
1	Перегляд літератури про питання роботи. Аналіз дослідження можливості випробування лазерового шоку.	06.10.2022–13.10.2022	
2	Встановити цифрову модель симуляції лазерового шоку, виберіть відповідний алгоритм, розмір сітки і час збільшення.	14.10.2022–24.10.2022	
3	Аналізовані оптимальні параметри процесу стіни та обмеження діри з однієї точки удару.	25.10.2022–01.11.2022	
4	Аналіз впливу співвідношення перекриття на залишкове поле стресу під декількох точок лазерового шоку.	6.10.2022–23.10.2022	
5	Виконання частин, присвячених захисту середовища і праці.	24.10.2022–31.10.2022	
6	Підготовка ілюстративного матеріалу, написання пояснювальної записки.	1.11.2022–7.11.2022	
7	Перевірка, редагування та виправлення пояснювальної записки.	7.11.2022–10.11.2022	

7. Консультанти з окремих розділів:

Розділ	Консультант	Дата, підпис	
		Завдання видав	Завдання прийняв
Охорона праці	к.біол.н., доцент Катериніа КАЖАН		
Охорона навколишнього середовища	к.т.н, доцент Леся ПАВЛЮХ		

8. Дата видачі завдання: 10 Сепня 2022 року

Керівник дипломної роботи _____ Вадим ЗАКІЄВ

Завдання прийняв до виконання _____ Jiayu HAO

NATIONAL AVIATION UNIVERSITY

Aerospace Faculty
Department of Aircraft Design
Educational Degree "Master"
Specialty 134 "Aviation and Aerospace Technologies"
Educational Professional Program "Aircraft Equipment"

APPROVED BY
Head of Department,
Dr. Sc., professor
_____ Serhiy IGNATOVYCH
«___» _____ 2022

TASK

for the master degree thesis

Jiayu HAO

1. Topic: « Numerical simulation of laser shock peening of titanium helicopter hub connector», approved by the Rector's order № 1861 «05» October 2022.
2. Period of work: since 05 October 2022 till 10 November 2022.
3. Initial data: Johnson-Cook constitutive model parameters of TB6 titanium alloy material.
4. Content: Analysis of the application of laser shock peening in aviation industry, an new multipoint algorithm is studied, analyze the optimal process parameters of single point impact hole wall and hole circumference, get the best multi-point overlap rate.
5. Required material: Laser power range, mechanical property parameters of TB6 titanium.

6. Thesis schedule:

№	Task	Time limits	Done
1	Review of the literature on the issues of work. Analysis of laser shock peening feasibility study.	06.10.2022–13.10.2022	
2	Establish numerical simulation model of laser shock peening, select appropriate algorithm, grid size and increment time.	14.10.2022–24.10.2022	
3	Analyze the optimal process parameters of single point impact hole wall and hole circumference.	25.10.2022–01.11.2022	
4	Analysis of the influence of overlap rate on residual stress field under multi-point laser shock.	06.10.2022–23.10.2022	
5	Execution of the parts, devoted to environmental and labor protection.	24.10.2022–31.10.2022	
6	Preparation of illustrative material, writing the report.	01.11.2022–07.11.2022	
7	Explanatory note checking, editing and correction.	07.11.2022–10.11.2022	

7. Special chapter advisers:

Chapter	Adviser	Date, signature	
		Task issued	Task received
Labor protection	PhD, associate professor Catarina KAJAN		
Environmental protection	Dr. Sc., associate professor Lesya PAVLYUKH		

8. Date of issue of the task: 10 September 2022 year

Supervisor: _____ Vadim ZAKIEV

Student: _____ Jiayu HAO

РЕФЕРАТ

Пояснювальна записка дипломної роботи магістра «Числова симуляція лазерового шокового мотузку з'єднальника з гелікоптером з титаном»:

72 с., 38 рис., 2 табл., 37 джерел

Об'єкт дослідження – Найкращі параметри лазерного шоку.

Предмет дослідження – Аналіз залишкового поля стресу гелікоптерного центру з лігацією Титану ТВ6 за допомогою лазерового шоку.

Мета магістерської роботи – Знайдіть ефективний метод заощадження лазерового шоку для матеріалу гелікоптерного головного шляху ТБ6, щоб покращити високий цикл відстань до втомлення.

Методи дослідження та розробки – Обчислити оптимальний діапазон крокового тиску хвилі шоку у процесі мочування, симулювати процес мочування лазерових шоків за допомогою Abaqus. Дінамічні виразні та статичні implicit ні алгоритми використовуються для аналізу закону варіації залишкового пол я стресу.

Новизна результатів – Стіна діри була підкріплена лазеровим шоком, і результати були порівняні з результатами обмеження діри.

Практична цінність – Аналізуються оптимальні параметри для лазерового шоку матеріалу з титанської легенди ТВ6, що надає теоретичну основу для обробки дір гелікоптерного центру, а також надає підтримку даних для справжнього обробки, ефективно покращуючи життя втомлення гелікоптерного центру.

Кваліфікаційна робота магістра, лазерне ударне клепання, титановий сплав, щільність потужності, залишкове напруження, щільність перекриття

ABSTRACT

Master degree thesis "Numerical simulation of laser shock peening of titanium helicopter hub connector"

72 p., 38 fig., 2 table, 37 references

Object of study – The best laser shock peening parameters.

Subject of study – Residual Stress Field Analysis of TB6 Titanium Alloy Helicopter Hub by Laser Shock peening.

Aim of master thesis – Find an efficient laser shock strengthening method for TB6 titanium alloy helicopter hub material to improve the high cycle fatigue resistance.

Research and development methods – Calculate the optimal peak pressure range of the shock wave in the peening process, simulate the laser shock peening process with Abaqus. The dynamic explicit and static implicit algorithms are used to analyze the variation law of the residual stress field.

Novelty of the results – The hole wall was strengthened by laser shock peening, and the results were compared with those of the hole circumference.

Practical value – The optimal parameters for laser shock peening of TB6 titanium alloy material are analyzed, which provides a theoretical basis for processing the holes of helicopter hub, and also provides data support for actual processing, effectively improving the fatigue life of helicopter hub.

Master thesis, laser shock peening, titanium alloy, power density, residual stress, overlap rate

CONTENT

INTRODUCTION

The hub material of the helicopter is TB6. When the blade part of the helicopter rotor system rotates continuously in the asymmetric flow field, adverse vibration and coupling load will occur. Under the harsh working environment, the hub connectors bear a large number of complex centrifugal forces, flapping bending moments and shimmy bending moments transmitted by the blades, and are subject to high frequency and low amplitude high cycle alternating fatigue loads for a long time. Therefore, fatigue fracture is easy to occur at the connection holes, which affects helicopter flight safety. Without changing the material properties and improving the service life and fatigue resistance of the connector, the surface strengthening treatment is usually carried out on the connection holes of key load-bearing components to introduce residual compressive stress field. But the traditional process cannot meet the expected processing requirements.

Laser shock peening is a surface strengthening process that uses a short pulse laser with high peak power density to irradiate the target, induce the generation of high-temperature and high-pressure plasma, and under the effect of the constraint layer, the shock wave pressure reaches the GPa level and diffuses inside the target, making the microstructure grain of the machined surface fine, producing plastic strain, and having a deeper residual compressive stress layer. At present, laser shock peening has been used by a large number of scholars at home and abroad to improve the fatigue performance of holes. Although many scholars have applied the laser shock strengthening technology to the hole strengthening process, the hole wall of the hole is the contact surface when the hole is in contact with the shaft or bolt, and most cracks originate here. However, many studies only focus on the strengthening of the hole surface to form an effective residual stress field on the hole wall.

The first part compares different types of surface strengthening processes, and describes their characteristics and working principles. A new surface strengthening technology of laser shock peening is proposed. The current application in aviation industry of laser shock peening technology is described.

The second part study the numerical simulation of TB6 titanium alloy by laser shock peening. A combination method of "Explicit dynamic + Implicit static" solver is adopted, which is suitable for multi-point impact reinforcement. Determined a geometric dimension of the model, and the model was simplified under the condition that it met the experimental requirements and did not affect the stress results. The optimal laser power density and energy range are calculated. After analyzing the mesh convergence of the single point enhancement of the simple model, the mesh size of the local refinement area was determined to be 100μm. Best solution time of the Explicit analysis step is determined to be 1500ns.

The third part focuses on the systematic study of laser shock strengthening. Within the reasonable range of power density, impact the material surface one by one, increase the overlap ratio of light spot, find the power density that can reach the maximum residual compressive stress and the deepest stress layer depth, and compare the two different impact parts of hole wall and hole circumference, and analyze the rule change of residual stress field.

The fourth part discusses the details of labor protection. In order to carry out experimental research on laser shock strengthening, engineers need a laboratory or workplace with complete equipment and in line with national health regulations. This puts forward requirements for many factors, such as experimental clothing, maintenance procedures, workplaces, etc. The harmful effects of laser on people in the process of experimental research are considered.

The last part, environmental protection, focuses on the negative impact of machining on the environment and biology, and the methods to solve these problems.

PART 1
LASER SHOCK PEENING FOR IMPROVEMENT MECHANICAL PROPERTIES OF SURFACE LAYER

Resistance to Fatigue fracture is an important factor affecting the safety and reliability of mechanical structure and equipment. In the use of aviation equipment, fatigue fracture has caused a lot of serious flight accidents, and the economic losses are also very amazing. Especially the high cycle fatigue fracture of aviation components is a difficult problem in development and use. However, the problem of high-cycle fatigue fracture of hole structure is a difficult problem in the development and operation aircraft systems and parts [1].

In order to improve the reliability and prolong the service life of structural parts under service conditions, technology of surface strengthening has been studied and applied more and more internationally without changing the quality of target material [2]. As a new technology of surface strengthening developed in the middle of last century, laser shock peening has been widely studied and developed rapidly in solving the fatigue fracture of aviation components. At present, the commonly used surface strengthening methods include mechanical shot peening, low plastic rolling, rolling, etc. [3]. But traditional way of surface strengthening is always with some shortcomings, especially in the area of holes of component reinforcement is always not satisfactory, such as after mechanical shot peening affected layer, shallow depth, the depth of residual compressive stress layer is small, cold work hardening rate is high, under the action of load and thermal instability, prone to relax, reduce the reinforcement effect [4]. However, the low-plastic rolling device needs to be specially designed for the reinforced parts, which has poor use flexibility and difficulties in the implementation of complex parts [5]. These methods have some disadvantages in strengthening hole.

It is well known that many parts in the aerospace field, such as aircraft engine blades, gear parts, fastening holes on aircraft skin, etc., are generally used under cyclic loading conditions, so their fatigue behavior in the working process is particularly important. A large number of studies have shown that fatigue cracks mostly originate from machining defects, surface defects or stress concentration parts of components, but not all fatigue cracks can be

attributed to these reasons. Through a large number of experimental studies have found that when the component under the effect of different sizes of stress of fatigue performance will be different, this kind of circumstance, explore the fatigue behavior of material under different stress level, on the reason of the fatigue fracture criterion, thus further take effective preventive measures has the decisive role.

1.1 Surface strengthening methods

Cold extrusion (Figure 1.1) is the plastic deformation of a hole by forcing a steel ball or cone rod with a diameter slightly larger than the hole through the hole (pulling or pressing). When the structural hole is subjected to external alternating load, the residual stress around the hole will offset part of the tensile stress, so that the maximum value σ_{Max} of the actual alternating load is reduced (the amplitude is unchanged), but the average stress is greatly decreased, as shown in Figure 1.2 Thus, the fatigue life of the structure is improved [6,7].

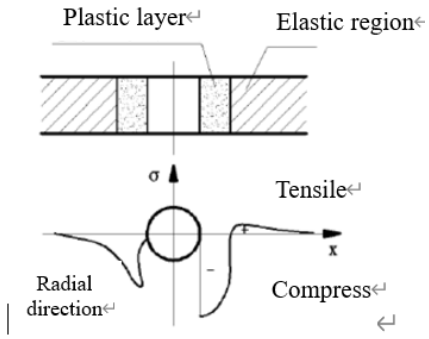

Figure 1.1 – Residual stress distribution in the surrounding of hole after cold extrusion

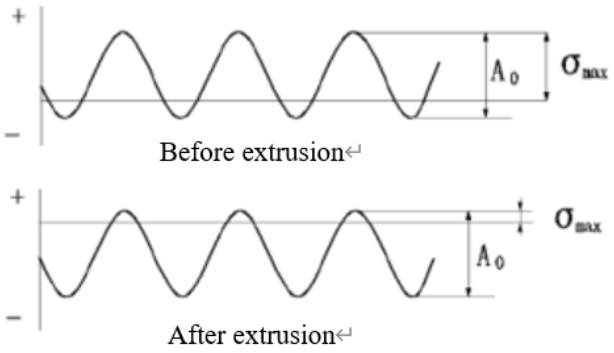

Figure 1.2 – Alternative stress around hole before and after cold extrusion

Hole *cold extrusion* strengthening way, direct cold extrusion of the mandrel - axial relative movement, the hole wall is easy to appear abrasion; Slit bushing cold extrusion - after extrusion hole wall formed a step, need to fill processing; The strengthening effect is stable and widely used; It has the advantage of multiple implementations. Main strengthening parameters: extrusion amount (involving initial hole aperture, bushing thickness, mandrel working end diameter, etc.), bottom hole hinging amount. Figure 1.3 is a schematic diagram of hole cold extrusion strengthening mode.

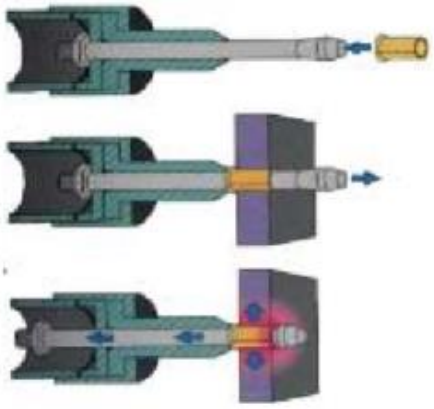

Figure 1.3 – Cold extrusion strengthening method of hole

Interference fit connection in the interference fit connection, pre-tension is generated at the hole edge. When the structure is subjected to cyclic external loading, the resultant peak stress and pretension may exceed the material yield limit. The peak stress with small change and the valley stress with large change can greatly reduce the stress amplitude and thus significantly improve the structure life. The tensile stress is formed between the hole wall and the fastener through a large amount of interference, and the fatigue resistance is improved at low and medium stress levels.

This technology is used for the key parts of the bearing structure without disassembly, the parts of the hole cold extrusion without access, such as interference bolts, high locks used for the beam butt end fastening holes, frame beam edge bar connection holes, interference riveting (crown rivet), but also used for the inlet skin connection holes.

In FIG. 1.4, during bushing installation, the manger squeezes the bushing along the radial direction to make the bushing expand along the radial direction (the bushing will also produce plastic deformation), and then deform the matrix material. After cold extrusion, the

matrix material will produce a springback, and the springback trend exceeds that of the bushing material, so that the bushing will be "held tight" and the residual compressive stress zone will be generated around the holes in the matrix. Under the action of alternating load, the stress amplitude around the hole of the matrix does not change, but the existence of residual compressive stress makes the average stress greatly decrease, thus prolonging the growth time of fatigue crack.

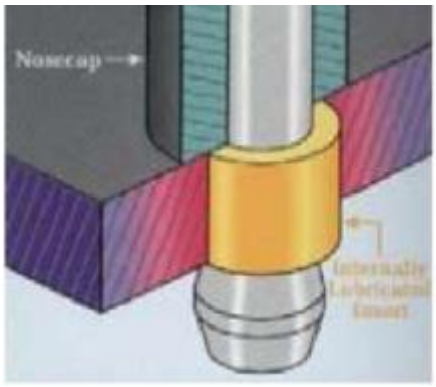

Figure 1.4 – Press fit bushing strengthening

Press fit bushing strengthening, according to the demand, can be designed, no shoulder, with shoulder, double with shoulder, etc., suitable for body material pressing bushing material. Suitable for small margin, improve the fatigue life and fatigue strength of the base metal structure, reduce the potential of the weight of the structure, the main process parameters: interference (relative and absolute interference), bottom hole diameter, mandrel working end diameter, hole edge distance and other decisions.

Shot peening is let the high-speed projectile constantly impinges on the surface of the parts [8,9], causing a series of complex metal cell changes on the surface of the parts, forming residual compressive stress and tiny grain dislocation, so as to achieve the purpose of improving the fatigue strength and stress corrosion resistance of the parts. Main process parameters: shot peening medium, shot peening strength, coverage; Shot peening medium includes projectile material (cast steel shot → glass shot → ceramic shot), projectile diameter; Shot peening strength includes projectile velocity and projectile kinetic energy, which is characterized by deformation of *Almen* test piece. The ratio of the area occupied by the projectile pit on the surface of the sprayed part to the total area of the sprayed surface has a basic coverage of 98%.

It is widely used in the structure of new aircraft body and landing gear of military and civil aircraft abroad, and some landing gear structures of military aircraft in China have applied this technology. Ceramic shot peening, to avoid the pollution of cast steel shot to aluminum and titanium, glass shot is vulnerable, ceramic shot peening is used in the military frame beam type thin-walled structure, in the newly developed military aircraft aluminum and titanium alloy material frame beam type ceramic shot peening is used in a small range.

1.2 Laser shock peening technique and its advantages

1.2.1 Laser shock peening technique

The basic principle of laser shock peening is: Nanosecond pulse laser with peak power density (>10^9W/cm^2) is used to irradiate the metal surface, so that the absorption protective layer coated on the metal surface absorbs laser energy and explosively vaporizes and evaporates, generating high temperature (>10^7K) and high pressure (>1GPa) plasma, which is constrained by the constraint layer. High pressure shock wave (GPa magnitude) is formed and propagated into the material, causing the dynamic cold plastic deformation of the material with ultra-high strain rate (>10^6/s), resulting in stable residual compressive stress and microstructure changes, and significantly improving the resistance to fatigue, wear and stress corrosion of the metal material [10,11], as shown in FIG. 1.5

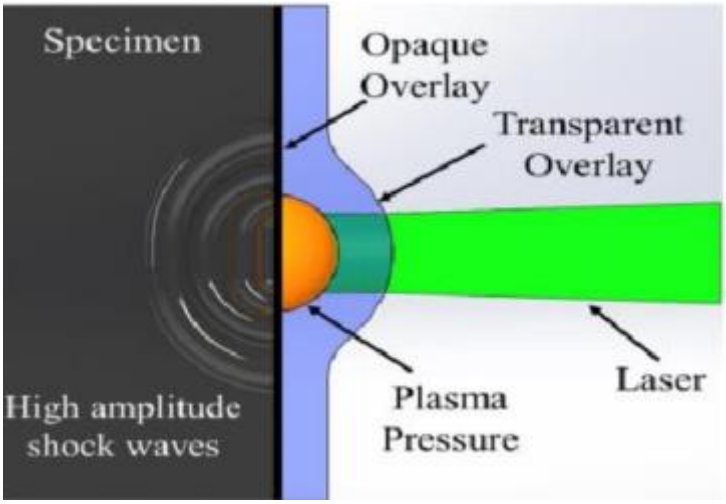

Figure 1.5 – The basic principle of laser shock peening

Laser shock peening equipment is mainly divided into three parts :(1) Laser optical path control system, as shown in FIG. 1.6(a); (2) Clamping and motion control system, as

shown in FIG. 1.6(b); (3) Flow control system, as shown in FIG. 1.6(c). In the laser shock peening process, the absorption layer is first covered on the material to be treated, generally using black paint or aluminum foil, and then a layer of restraint layer is covered above the absorption layer, generally using deionized water (generally running water) or glass that is transparent to the laser beam. Then, the absorption layer is illuminated by a laser beam with high energy density and short pulse. The absorption layer generates high-pressure plasma and expands rapidly, forming shock wave. The existence of the confinement layer will promote the shock wave to propagate into the material, and the peak of the shock wave will gradually decay during the shock wave propagation. On the surface of the material, the peak value of the shock wave will exceed the dynamic yield strength of the material, resulting in elastic-plastic deformation. However, in the subsurface layer and the core of the material, the peak value of the shock wave will not exceed the dynamic yield strength of the material due to attenuation in the propagation process, so the surface layer and the core of the material are always in elastic deformation. When the shock wave load disappears, the elastic deformation can be recovered. At this time, the surface and internal materials contract at the same time, while the plastic deformation cannot be recovered. Therefore, the residual compressive stress field will eventually be generated on the surface of the material, and the residual tensile stress field will be generated on the subsurface and the core of the material.

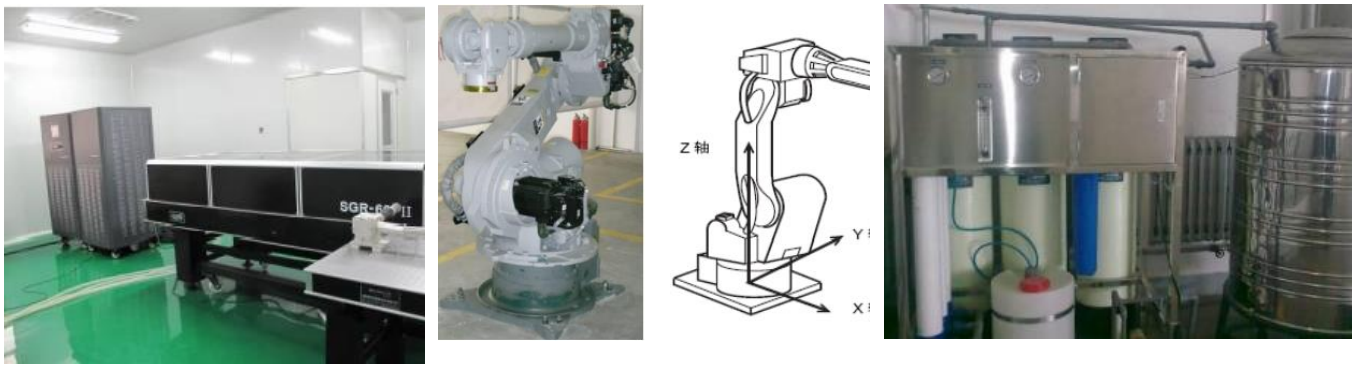

a) Laser control system b) Clamping and motion system c) Flow control system

Figure 1.6 – Laser shock peening equipment

Laser shock peening uses laser-induced plasma shock wave to increase the shock wave pressure through the restraint layer, and then constitutes the absorption protective layer

and the restraint layer structure. This structure is typical and has the following three characteristics

(1) High pressure. The detonation pressure is on the order of several GPa, TPa. This is difficult to achieve conventional mechanical processing, such as mechanical stamping pressure is often between dozens of MPa to hundreds of MPa.

(2) High energy. The laser beam single pulse energy reaches tens of J, the peak power reaches GW magnitude, and the light energy is transformed into the mechanical energy of shock wave within 10~30ns, which realizes the efficient use of energy.

(3) Ultra-high strain rate. The shock wave action time is only tens to hundreds of nanoseconds, and the strain rate reaches $10^6 s^{-1}$, which is 10,000 times higher than mechanical stamping and 100 times higher than explosive forming. It is a manufacturing method under extreme conditions in extreme environments.

1.2.2 Laser shock peening advantages

High-power pulsed laser irradiation on the surface of the material (surface coating) makes it rapidly vaporize and generate plasma, which expands and explodes to form shock waves propagating inward. Plastic deformation occurs on the surface of the material to form an impact strengthening layer and a residual compressive stress layer, which improves the local fatigue fracture resistance of the metal material. The main process parameters of laser shock peening are: absorbing layer material, restraint layer, laser energy or power density, impact times, impact sequence, etc. [12]

The development of strong lasers at home and abroad provides space for the application of surface laser shock peening, [13-15]. Aircraft F22 main frame outer transition zone edge surface laser shock peening, domestic titanium alloy blade fatigue weak zone laser shock peening application (tip, blade root), aluminum alloy small hole (Φ2.6mm) laser shock peening application research and small-scale installation application, Application of laser shock peening in stress concentration zone of skeleton (Al-Ti alloy) parts [16].

Laser shock peening and surface hardening, surface chemical heat treatment and mechanical shot peening, hammer, cold extrusion, rolling method, compared with its unique advantages: 1) due to the nanosecond laser shock action time is very short, and the

workpiece surface coating absorbing layer (layer and heat resistance), laser and coating of the shock wave is induced by interaction force effect. 2) With superposition and cleanliness, multiple shot peening can meet the requirements of improving the material strengthening effect and selecting the strengthening area, and it is a clean process technology without deposition pollution and infiltration. 3) Ultra-high pressure and high strain rate, the pressure of the shock wave can reach GPa or even TPa, and the strain rate can reach $10^6 s^{-1}$, which is an extreme manufacturing method under extreme conditions. 4) Laser parameters, trajectory and focus spot size are precisely controllable, with process repeatability, especially for fatigue parts with local stress concentration, such as slots, holes, corners and rounded corners that are prone to fatigue damage. Compared with traditional surface strengthening techniques such as mechanical shot peening, rolling and cold extrusion, laser impact strengthening has obvious technical advantages [17].

1.3 Applications of laser shock peening

Due to special advantages in the process of laser shock peening in manufacturing, many countries in the world of laser shock peening research, from different aspects to promote the technological progress, and NASA in the United States in 2008, 2010, San Francisco and Osaka, Japan in 2012, held the three laser shock peening international academic conferences. French research focuses on laser shock peening mechanism, and its important contribution is to further develop the theory of laser-induced shock wave [18,19]. Laser shock peening was used in Japan to solve the corrosion problem of nuclear reactor components [20]. In addition, scholars from Spain, Australia, Germany, India and other countries have also carried out relevant studies from the numerical simulation of laser shock peening [21], shock wave testing, and material microstructure analysis [22], but only the United States and China have really applied them in large-scale engineering. The United States took the lead in achieving large-scale application in the aviation industry [23,24] (the United Kingdom adopted the equipment and technology from the United States), and listed as the key technology of the engine of the fourth generation fighter aircraft. At present, the applications of laser shock peening are mainly concentrated in the aircraft engine fan/compressor blade, helicopter transmission gear, aircraft hook, nuclear waste container

weld, weld nuclear fuel rods shell, large gas turbine, turbine blades, and car key parts such as the cold end components, and in the application research of helicopter hub parts rarely reported.

The development history of laser shock peening is closely related to the fatigue fracture resistance of aero-engine components. Aiming at the problem of high cycle fatigue fracture of aero-engines, in 1994, the United States began to implement the "High cycle fatigue science and technology program", whose goal was to improve the high cycle fatigue design level of components, eliminate the aero-engine failures caused by high cycle fatigue, improve flight safety and reduce the use cost [25,26]. "High cycle fatigue science and technology program" divides the technical work into 7 action groups [27] :(1) component surface treatment; (2) Study on material damage tolerance; (3) Testing; (4) Component analysis; (5) Estimation of forced response; (6) passive damping; (7) Engine validation (added in 1999). Among them, the Component Surface Treatment Action Group provides coordination and linkages between participants engaged in laser impact peening and related technologies, with the goal of increasing the blade leading edge damage tolerance by a factor of 15 (allowable crack length from 0.127mm to 1.905mm). The component surface treatment action group selected from many surface strengthening technologies, focusing on the development of laser shock peening technology, as the primary process technical measures, Organized Lawrence Livermore National Laboratory, Los Alamos National Laboratory, the United States Air Force Research Laboratory, GE Company (General Electric Company), MIC Company (Metal Modification Company) and other units to jointly tackle key problems, after a large number of tests, The results show that laser shock peening is one of the effective means to solve the problem of high cycle fatigue of aero-engine. The ultimate goal of this group is to develop and realize the capability of production laser shock peening, which can meet the economic endurance target of the American military and manufacturers for fatigue key parts. In February 1995, Dr. Jeff Dnlaney, who participated in the program, founded LSPT (Laser Shock Peening Technology), the world's first company engaged in the application of laser shock peening technology. It was the National Research Program on High Cycle Fatigue that pushed laser shock peening from the laboratory to industrial applications.

Based on the research results of National Research Program on High Cycle Fatigue, since 1995, the United States began to study the problems of F101 engine in the Gulf War, such as the insufficient ability of first-stage fan blades to resist foreign object damage, and adopted laser shock peening technology to improve the blade edge damage tolerance, requiring that the blade edge damage tolerance be increased by 15 times. That is, the allowable length of small cracks extends from 0.127mm to 2mm. GE has shown through tests that: The first stage fan Ti-8Al-1V-1Mo blade (Chinese metal code TA11) of F101 engine can greatly improve the damage tolerance of external materials after laser shock peening (as shown in Figure 1.7). When the crack length reaches 6.35mm (impact simulated damage) /3.175mm (EDM simulated damage), the fatigue strength of the blade can still reach or exceed the new blade fatigue strength level.

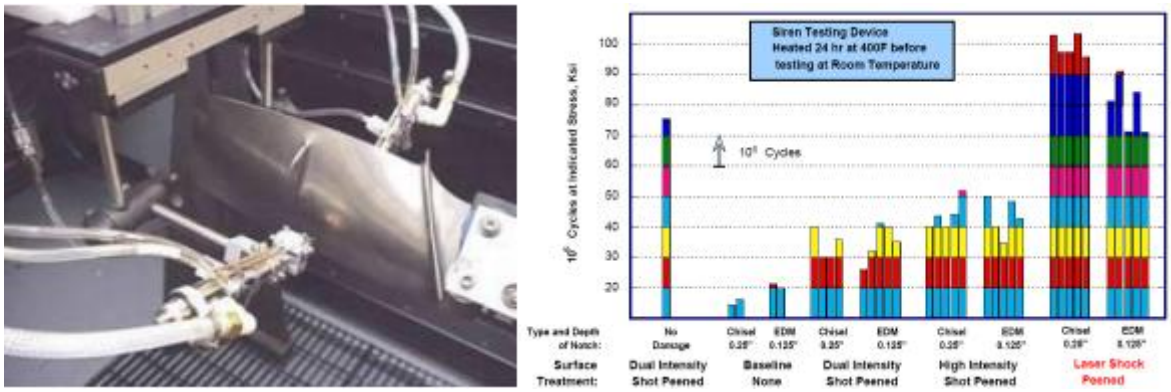

Figure 1.7 - Laser shock peening and damage tolerance data of F101 engine first fan blade

From 1998 to 2000, American GE Company applied laser shock peening technology to strengthen F110 and F404 engine fan blades and compressor blades, and solved the problem of high-cycle fatigue crack fracture of F110 and F404 engine fan blades. And the ability of these engines to resist foreign material damage was increased by 15 times [28]. Figure 1.8 shows the application of laser shock peening technology in several types of aircraft/engines by GE.

Figure 1.8 - GE Laser shock peened aircraft/engine components and quantities

In 2000, at the late stage of the development of F119 engine, it was found that its fourth stage integral blade disc's resistance to external material damage did not meet the requirements of F/A-22 aircraft, and it was necessary to raise the threshold value of stress intensity factor by more than three times at least. It would take A lot of time and money to redesign it. Therefore, PW and The U.S. Air Force proposed a technical requirment to enhance F119 engine fourth stage intergral disc resistance to external material damage using laser shock peening. LSPT and Pratt & Whitney Corporation of the United States used laser shock peening technology to process the cracked integral blade and disc blade. The blade material was Ti6-Al4-V, the length of prefabricated blade crack was 0.127mm, and the original blade fatigue strength was 586.1-689.5MPa, which decreased to 206.85MPa after damage. It is far below the design requirement of blade (379MPa). After laser shock peening, the fatigue strength of the damaged blade rises to 413.7mpa again. The experiment shows that laser shock strengthening can more than double the fatigue strength of the notched blade disc, and great success has been achieved [29]. The U.S. Air Force has allowed LSPT to perform laser shock peening of the entire blade disc, which would cost tens of millions of dollars to redesign and replace and would significantly delay development and production. Therefore, laser shock peening has been listed as one of the key technologies of engine development of the fourth generation fighter aircraft by the United States, which is not only used to improve the anti-injury ability of blades, but also used to improve the high-cycle fatigue strength and damage repair performance of blades.

Since 2002, laser shock peening has been widely used in the manufacture and repair of aviation components in the United States. The fretting fatigue life of Qieer blade

reinforced by laser shock was increased at least 25 times by LSPT. According to MIC, laser shock peening for jet engine blades production [30], improved reliability, because of the decrease blade replacement, a month can save the U.S. Air Force aircraft maintenance cost and parts replacement cost millions of dollars, is expected to the processing of military engine blades, can save the cost more than 1 billion dollars. In 2005, MIC received the Highest Achievement Award for Defense Manufacturing in the United States for its contributions to laser shock peening.

In order to solve the problem of fatigue fracture of carrier aircraft landing hooks, the United States Naval Air Warfare Center War minster, Metal Improvement Corporation, and Technical Cooperation Center jointly tackled key issues and used laser shock peening and traditional shot peening to strengthen the simulated hook components (low alloy and high strength steel) [31]. The Second International Conference on Laser Peening. Francisco. 19~21, April, 2010. The experimental results show that both laser shock peening and shot peening can effectively prolong the propagation life of fatigue cracks, and the effect of laser shock peening is much better than shot peening because of the introduction of deep residual stress field. The service time of the component can be greatly extended by laser shock peening after the hook has been used for a certain time. In 2010, it was popularized and applied in T45 aircraft parts. Aiming at the problem of insufficient fatigue strength of bolt holes connecting the wings and fuselage of F-22 aircraft, the United States carried out related research and realized laser shock peening of this part. The production line construction was up to 100 million dollars.

In the treatments of welds, laser shock peening is used for welding manufacturing and damage repair of engine components, eliminating residual tensile stress, preventing stress corrosion and improving fatigue strength [32,33]. In addition, from 2000 to 2002, Lawrence Livermore National Laboratory demonstrated that laser shock peening can significantly reduce stress corrosion and crack growth rates in welds. The nuclear waste storage container of the United States is deeply buried under the Yucca mountain, and it is required to be kept for 10,000 years without leakage. However, due to the residual tensile stress in the weld of the container, crack initiation, expansion and accelerated corrosion are caused. Experimental studies have proved that laser shock peening can greatly reduce the stress corrosion and

crack propagation of welds, and the technology has been applied to weld strengthening of nuclear waste containers in the United States (As shown in FIG. 1.9).

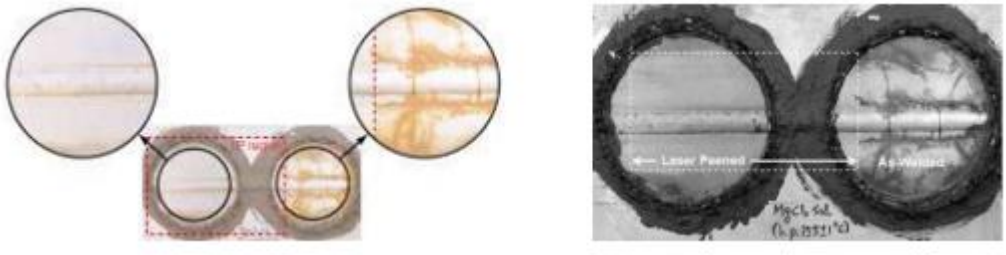

Figure 1.9 - Laser shock peening enhances stress corrosion resistance of metal
(Right figure is enlarged from left figure)

In civil aviation engine, laser shock enhancement technology was approved by Federal Aviation Administration and Japan Asia Airways as critical aircraft/engine maintenance technology in 2003, and has been successively applied to the manufacture and repair of engine blades such as CFM-56 of Boeing 737 aircraft and GE90 of A380 aircraft. After 2005, it was gradually extended to the treatment of large gas turbines (such as GE 7F gas turbine), water turbine blades, and key parts of automobiles, and achieved great economic benefits.

The Army has a pressing need to increase the power of helicopter engines (especially for use at high altitudes in Afghanistan), which requires a significant increase in the fatigue strength of the spindle and engine transmission components. The Army's Manufacturing Technology program uses laser shock peening to improve the fatigue strength of helicopter power and transmission units, including the Apache, Black Hawk and Chinook. Helicopter equipment manufacturers OEM, Boeing and Rolls-Royce took part in the research. The U.S. Army Manufacturing Technology Program mainly conducts laser shock peening gear and carburizing hardening research to verify the effectiveness of the technology and put it into parts production.

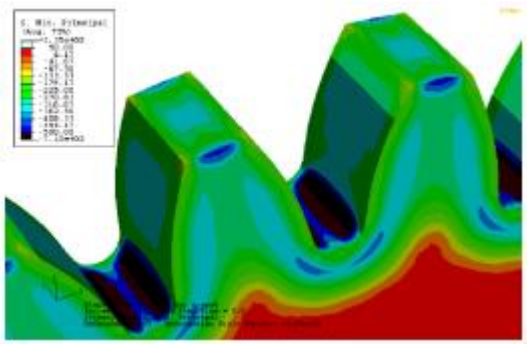

Figure 1.10 - The residual stress distribution after laser shock peening gear

Conclusion to the Part 1

At present, laser shock peening has obvious advantages over traditional surface strengthening process, which is suitable for widely used in aviation industry. However, domestic and foreign scholars have more research on laser shock peened plate, and less research on hole. In the contact between the hole connector and the shaft, the hole wall is the contact surface, where cracks often occur. It is difficult to form compressive stress at the hole wall only for laser shock peen the hole surface. Therefore, it is of great significance to carry out research on laser shock peening of thick hole wall for prolonging the life of helicopter hub under high cycle fatigue strength working environment.

PART 2
THE BASIS OF NUMERICAL SIMULATION OF LASER SHOCK PEENING

The process of laser shock intensification is a complex process involving the coupling of acoustic field, electromagnetic field, stress field and other fields, and each field affects each other. If a single experiment is used to verify the results, the experimental period is long, the steps are tedious and the cost is huge, which cannot meet the needs of modern processing. Numerical simulation of laser shock intensification is to establish the exclusive constitutive model according to the real physical and chemical characteristics of the material through simulation software, the corresponding model grid is reasonably divided, the pressure model of laser shock wave is loaded, and the corresponding boundary conditions are set to obtain the change rule of the whole process, so as to facilitate the experimental research. Compared with experimental research, numerical simulation has higher requirements on theoretical basis, short calculation period, low cost, and is convenient to study the laser shock wave propagation process at a specific time. Therefore, numerical simulation research is the premise of experimental research. In this chapter, based on Abaqus software, the numerical simulation process of laser shock strengthening TB6 titanium alloy is analyzed and discussed.

2.1 The finite element algorithm

In 1999, Braisted et al. [34] carried out numerical simulation of laser shock peening on titanium alloy Ti-6Al-4V and stainless steel 35CD4, and analyzed the propagation process of laser shock wave in the material and the distribution of residual stress field. The simulation results were compared with the experimental results, and the error was within a controllable range, and the feasibility of numerical simulation on laser shock strengthening was obtained.

2.1.1 Explicit and Standard algorithm

The solver of Abaqus software has two main modules, *Abaqus/Standard* and *Abaqus/Explicit*, which have their own unique characteristics and scope of application for

different problems, and the analysis results of the two can be used as the initial conditions for solving each other to continue the calculation. In this way, the advantages of different solver modules in their respective fields can be fully played in the face of complex problems.

The time integrals of the *Explicit* and *Standard* solution procedures are shown in the following equation

$$\boldsymbol{M\ddot{u} = P - I} \tag{2.1}$$

In the equation (2.1), $\boldsymbol{M}$ -- mass matrix, $\boldsymbol{P}$ -- external force, $\boldsymbol{I}$ -- internal force of element, $\boldsymbol{\ddot{u}}$-- acceleration of node. Both explicit and standard solvers take node acceleration as the solution target to calculate the internal force of the unit, and the biggest difference lies in the solution method of node acceleration.

Abaqus/Standard uses implicit algorithms to analyze static, dynamic, thermal responses and conventional linear processes. Abaqus/Standard automatically increments based on Newton iteration method. At the end of $t + \Delta t$ increment step, the immediate displacement is calculated under the condition of satisfying the dynamic equilibrium. In this case, if the computational model is too large or contains some nonlinear conditions such as friction and impact, the quadratic convergence often requires a large number of iterations and may even fail to converge.

Abaqus/Explicit is widely used in the simulation of transient processes such as explosion and impact by using explicit algorithms [35]. It also has certain advantages in dealing with nonlinear problems. Abaqus/Explicit uses the central difference method, where the state at the end of the incremental step is based solely on the initial velocity, acceleration, and displacement of the incremental step, i.e.

$$\boldsymbol{\ddot{u}|_{(t)} = (M)^{-1} \cdot (P - I)|_{(t)}} \tag{2.2}$$

The advantage of Abaqus/Explicit is that the result can be obtained in small incremental steps in a short time, instead of having to solve the coupling equation one by one at each incremental step; At the same time, when the mass matrix is diagonal, there is no need to invert the mass matrix to solve the difference equation, and the calculation can be completed by matrix multiplication, which is very efficient.

2.1.2 Multi-point impact simulation algorithm

Since the laser loading time in laser shock peening is only nanosecond, the *Explicit* solver is suitable for laser shock initial loading and can determine the final residual stress field, but it takes too long to converge to the steady state. The *Standard* solver can also directly solve the whole process of laser shock intensification, but the disadvantage is that the grid division should not be too fine, because the solving process needs to calculate a large set of equations at each iteration, and the solving process is too long and the result error is large because the grid is not fine.

Traditionally, the combination of "Explicit dynamic + Implicit static" is adopted. Firstly, *Explicit* dynamic is used to simulate the laser shock loading process, and then *Standard* implicit static is used to simulate the rebound process of the specimen after laser shock and the distribution of stable stress field formed on the specimen. In this paper, *Explicit* solver will be used to complete multiple continuous shocks, and then *Standard* solver will be used to analyze the residual stress for rebound.

As shown in Figure 2.1, this optimized calculation method is different from the traditional point-by-point repeated explicit and implicit conversion method. It does not need to import stress and strain values between the explicit and implicit solvers and change the impact point coordinates in the Fortran subroutine VDLOAD at the same time for every impact. You only need to import the stress data after multiple points of continuous impact from the explicit and implicit mode once, as shown in Figure 2.2, which greatly saves resources and improves computing efficiency.

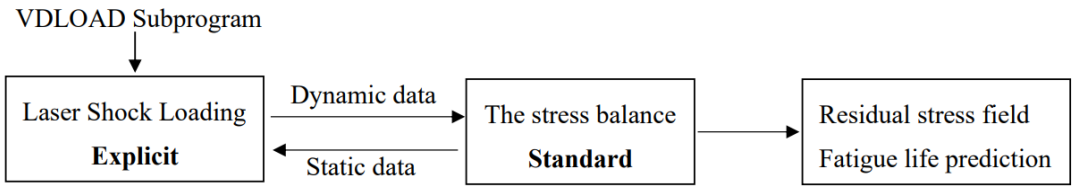

(a) Traditional simulation process

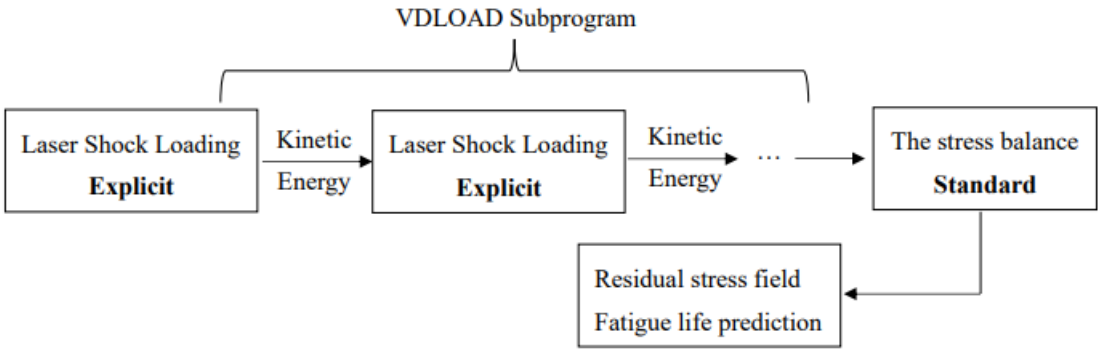

(b) Optimized simulation process

Figure 2.1 - Simulation process of laser shock peening

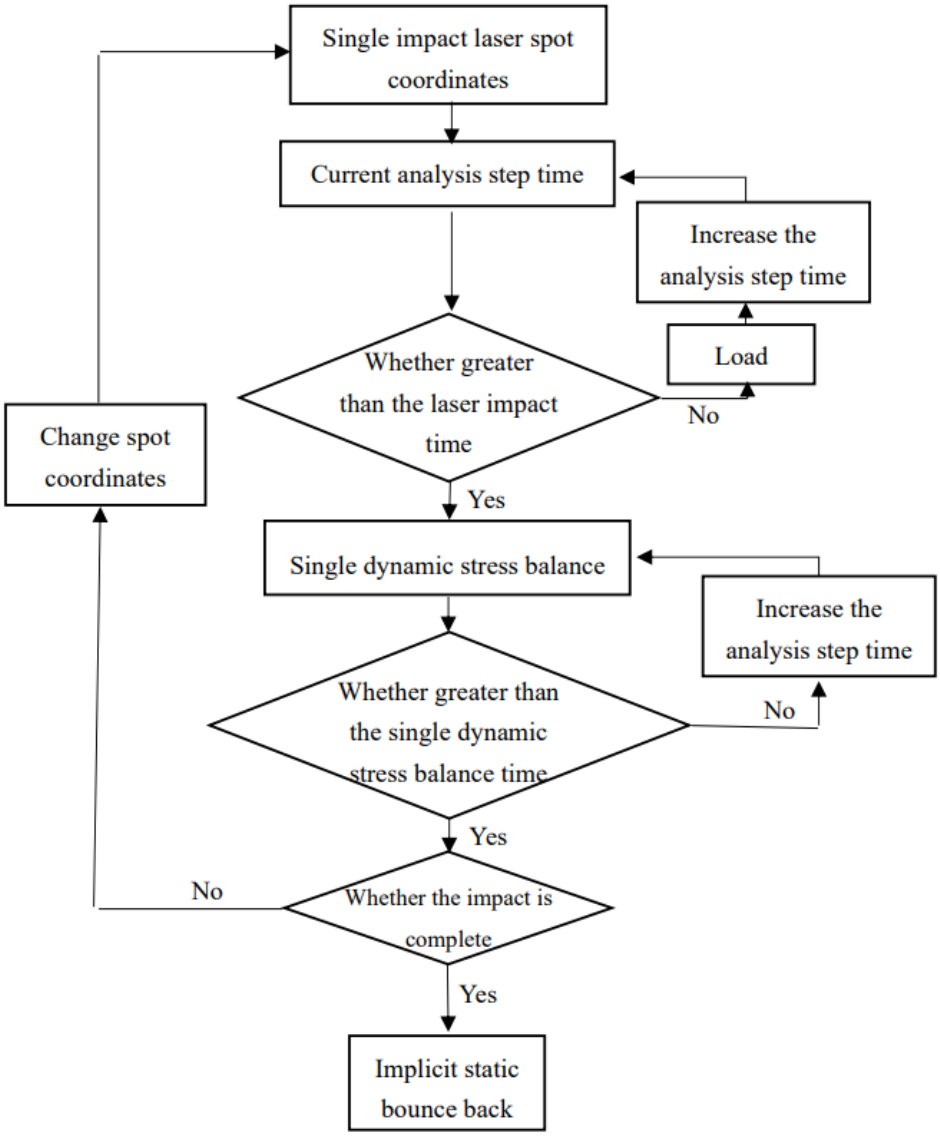

Figure 2.2 - VDLOAD subroutine loading process

2.2 Constitutive model of TB6 titanium alloy

This paper aims to study the strengthening method of hub connection hole of helicopter propeller. The target material is TB6, which is a β-type titanium alloy forged locally on the basis of Ti-1023. It has the advantages of high specific strength, low forging temperature, good fracture toughness, etc. The nominal component is Ti-10V-2Al-3Fe, and the main components are shown in Table 2.1.

Table 2.1 – The main components of TB6 titanium alloy

Al	V	Fe	C	N	H	Y	O	Ti
2.7	10	1.7	≤0.05	≤0.05	≤0.015	≤0.005	≤0.13	Bal.

The constitutive model is the stress-strain model of material, which reflects the dynamic response of material under load, and is the basis of numerical simulation of the dynamic response of target material. At present, according to the accumulation of engineering experience and experimental results, the *Elastic Perfectly Plastic* model, the *Zerilli-Armstrong* model, the *Johnson-Cook* model and the *Cowper-Symonds* model have been put forward to describe the constitutive equations of materials with high strain rates.

The *Elastic Perfectly Plastic* model is an ideal elastic plastic model that only considers the yield limit and excludes the factors of cold working hardening. It is assumed that the yield limit of raw material will undergo plastic deformation when the peak pressure is less than the yield strength, and no plastic strain will occur when the peak pressure is less than the yield strength. The *Zerilli-Armstrong* model is based on the deformation mechanism of material crystal and the unstable factors such as crystal dislocation, and a large number of parameters in the model need to be supported by experimental data. *Cowper-Symonds* model is an elastic linear reinforcement stress model. The *Johnson-Cook* model comprehensively considers the material strain rate, cold-working hardening, temperature and other factors, ignores the influence of material deformation and shock wave pressure, and ensures the accuracy on the premise of reducing the difficulty of obtaining relevant parameters. Therefore, *J-C* model is widely used at home and abroad to solve the simulation of high strain rate rapid loading problems such as high-speed impact and explosion impact. In this paper, considering the characteristics of strain rate as high as $10^6 s^{-1}$ in the process of

laser shock strengthening, *J-C* model will be adopted to simulate TB6 material, and the expression is shown in Equation (2.3):

$$\sigma = (A + B\varepsilon^n)[1 + C * \ln\left(1 + \frac{\dot{\varepsilon}}{\dot{\varepsilon_0}}\right)](1 - \frac{T - T_r}{T_m - T_r}) \tag{2.3}$$

Because the laser impact speed is very short, it heats and cools quickly, and the absorption protective layer coated on the surface absorbs the heat energy of the laser, laser impact strengthening belongs to cold processing, and the influence of thermal effect on residual stress can be ignored. Equation (2.4) can be simplified as follows:

$$\sigma = (A + B\varepsilon^n)[1 + C * \ln\left(1 + \frac{\dot{\varepsilon}}{\dot{\varepsilon_0}}\right)] \tag{2.4}$$

In Equation (2.4), *A, B, C* and *n* are all constants, respectively representing material yield strength, work hardening modulus, strain rate strengthening parameter and hardening coefficient. ε is the equivalent plastic strain, and $\frac{\dot{\varepsilon}}{\dot{\varepsilon_0}}$ is the non-dimensional plastic strain rate. Table 2.2 shows the parameters of J-C constitutive model for TB6 titanium alloy.

Table 2.2 – TB6 titanium alloy Johnson-Cook model parameters

ρ/(kg·m^{-3})	E/GPa	*v*	A/GPa	B/GPa	*n*	C
4620	102	0.33	797.5	574.4	0.1077	0.01

2.3 Geometric dimensions of model

TB6 is often used as the material of helicopter hub connectors. These connectors generally have the characteristics of large hole diameter and hole depth. These characteristics should be taken into account in the design of samples. The laser shock peened TB6 titanium alloy thick hole parts are shown in Figure 2.3. In order to improve the calculation efficiency, the hole is cut into 1/2, the hole radius is *r*=10mm, the hole depth is

10mm, and the chamfer is *C*1. According to the impact part, it can be divided into hole circumference (Figure 2.4 (a)) and hole wall (Figure 2.4 (b)).

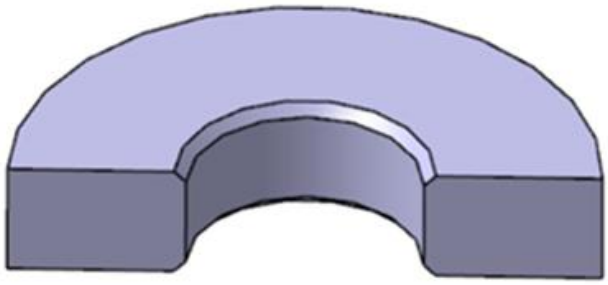

Figure 2.3 - TB6 titanium alloy hole model

(a) hole circumference (b) hole wall

Figure 2.4 - Schematic diagram of impact area

2.4 Shock wave pressure model

In order to ensure the effect of laser shock peening, it is necessary to estimate the laser power density selection range. Studies have shown that, the Hugoniot Elastic Limit (σ_{HEL}) of TB6 titanium alloy is expressed as

$$\sigma_{HEL} = (\frac{K}{2G} + \frac{2}{3})\sigma_{0.2} \tag{2.5}$$

In Equation (2.5), *K*--volume modulus, *K*=100GPa; *G*--shear modulus, *G*=38.3GPa; $\sigma_{0.2}$--yield strength, $\sigma_{0.2}$=1090MPa. The dynamic elastic limit σ_{HEL}= 2.15Gpa.

French scholar Fabbro et al. proposed the semi-empirical formula of laser shock wave peak pressure *P* and laser power density *I*:

$$P = 0.01\sqrt{\frac{\alpha}{2\alpha+3}}\sqrt{Z}\sqrt{A \times I} \tag{2.6}$$

$$\frac{3}{Z} = \frac{1}{Z_1} + \frac{1}{Z_2} + \frac{1}{Z_3} \tag{2.7}$$

In Equation (2.6), P is the peak pressure (GPa) of the shock wave; α -- efficiency coefficient. In this paper, the constraint layer is water and the absorption layer is black tape, so α=0.25; Z -- reduced acoustic impedance of water, black tape and target material, in Equation (2.7), Z_1 -- TB6 titanium alloy acoustic impedance, Z_2 -- constraint layer acoustic impedance, Z_3 -- absorption layer acoustic impedance, $Z=0.93\times10^6 g/(cm^2\cdot s)$; A -- energy absorption rate of the absorption layer. When the absorption layer is black tape, A=0.87; I -- laser output power density (GW/cm^2). When the shock wave pressure P reaches 2.0 ~2.5 times the metal dynamic elastic limit, the impact effect is the best, so the power density is selected in the range of 4.8~7.6 GW/cm^2.

$$I = \frac{4E}{\pi d^2 \tau} \tag{2.8}$$

In Equation (2.8), E -- laser energy; d -- spot diameter. This paper adopts a circular spot with a diameter of 3mm; τ -- pulse width, laser pulse width is 20ns. The calculation shows that the laser energy range corresponding to the power density is 6.8J~10.8J.

2.5 Model meshing

The accuracy of numerical simulation results is highly dependent on the meshing accuracy, and the high-speed dynamic response process of laser shock intensification has more demanding requirements on the mesh density than the ordinary dynamic process. When the mesh size of the finite element model is divided into smaller size and denser density, the calculation result will be more stable. However, blindly pursuing the finer mesh density partition will only multiply the computing time, reduce the computational efficiency, and put forward a major test to the computer performance. Therefore, the convergence analysis of the mesh is carried out, the mesh density is reasonably planned, and the mesh size is optimized to ensure the accuracy of the results and improve the computational efficiency at the same time.

In this section, a simple cuboid finite element model of 10×10×10mm with a circular spot diameter of 3mm was established to analyze the influence of mesh density on the numerical simulation of TB6 titanium alloy during laser shock peening. The center 6×6mm area is divided into five different mesh sizes: 200μm, 150μm, 120μm, 100μm, and 80μm, as

shown in Figure 2.5. The element type is C3D8R, which is a three-dimensional hexahedral eight-node subtraction integral element.

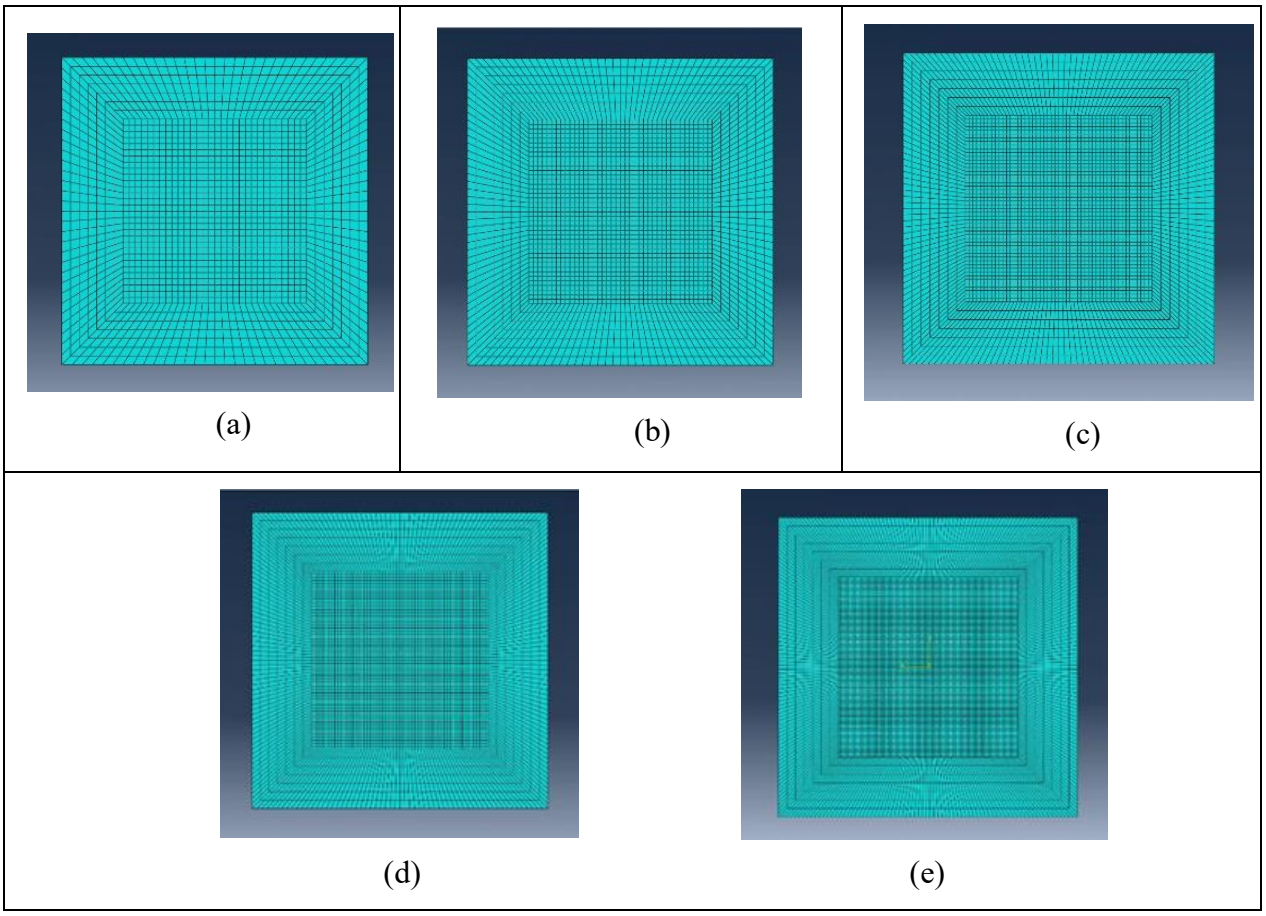

Figure 2.5-Meshing: (a) 200μm; (b) 150μm; (b) 120μm; (c) 100μm; (d) 80μm;

After calculation, it can be obtained that the same impact pressure, the residual stress values along the Y direction are also different with different grid densities. The residual stress field cloud diagram is shown in Figure 2.6. Obviously, the higher the grid density, the smoother the transition of stress field changes and the more intuitive display of stress wave diffusion process.

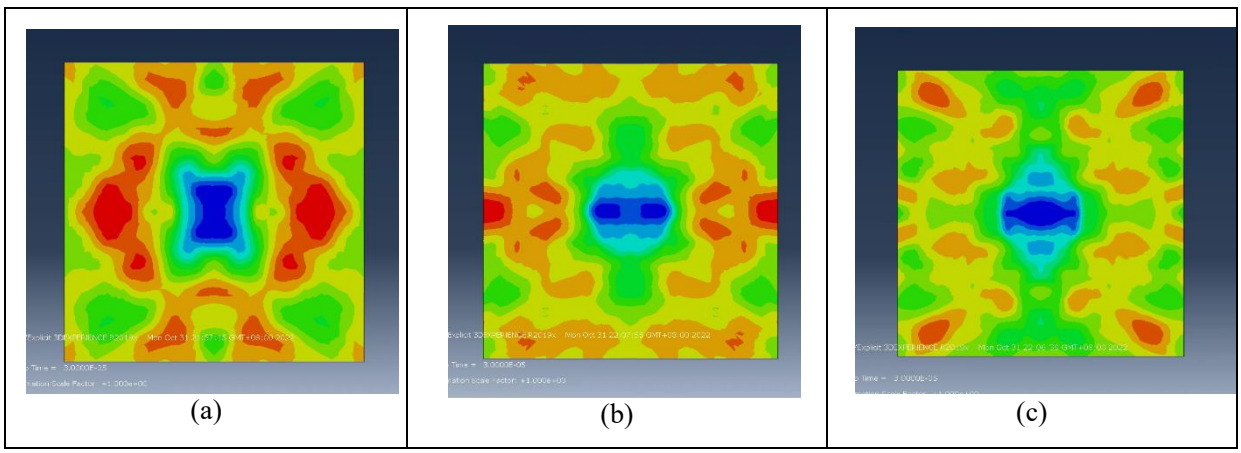

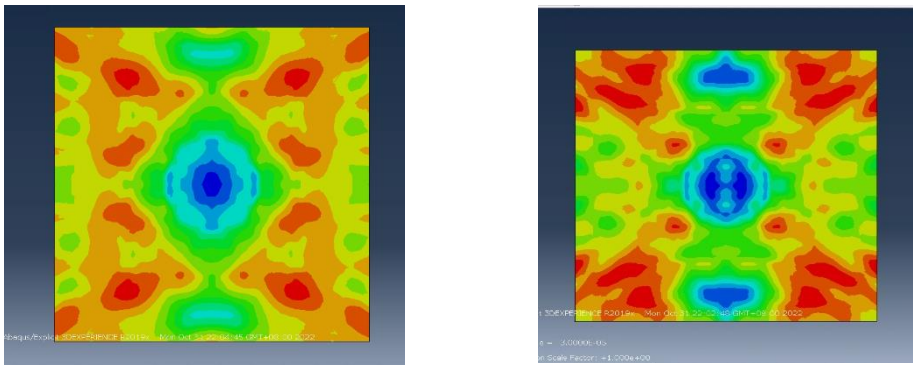

Figure 2.6- Residual stress of different mesh sizes: (a) 200μm; (b) 150μm; (b) 120μm; (c) 100μm; (d) 80μm;

By comparing the residual stress values calculated by different mesh sizes in Figure 2.7, it can be concluded that when the mesh size is 120μm, 100μm and 80μm, there is little difference in the finite element analysis results. Therefore, the minimum size of the local mesh refinement area of the model is selected as 100μm in the subsequent sections of this paper to obtain a better convergence stress field.

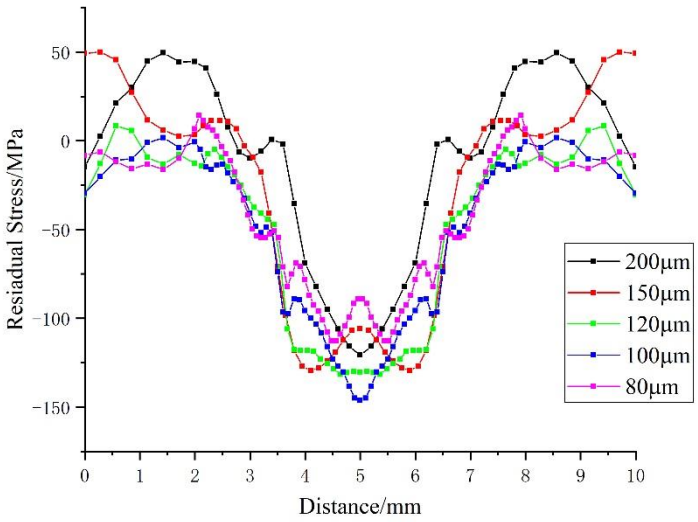

Figure 2.7- Analysis of mesh convergence

2.5 Analysis step time

When using Abaqus numerical simulation of laser shock peening, due to the laser shock loading time is too short, so to solve the time length and incremental step to finally has great influence on the data accuracy, long if incremental step length, impact on the two

steps calculation time interval is loaded, if the incremental step length too short, the number of iterations will index increase. If the solution time is too short, the whole elastic springback process cannot be calculated. If the solution time is too long, even if the calculation of the whole elastic springback process is completed, the efficiency is not high, especially in the simulation of multi-point impact, which has significant shortcomings.

According to the different material characteristics and laser process parameters, the simulation solution time is different. Wang Bohan et al. [36] determined that the solution time of single impact was 3000ns by numerical simulation of TC4 titanium alloy based on the energy change after single point impact. K Ding et al. [37] performed laser shock on 35CD430HRC alloy. When the solution time reached 4000ns, the variation range of the stress field of the material gradually converged and fluctuated within a fixed value range.

In order to obtain the stable explicit solution time of TB6 material, the material kinetic energy and internal energy change curves under impact were extracted, as shown in Figure 2.8. When the time is between 0 and 60ns, the energy of the material rapidly reaches the maximum value in a short time, and then gradually weakens, and the energy tends to be stable at 1500ns. Therefore, it can be determined that the single dynamic solution time is 1500ns, which can improve the computational efficiency on the premise of ensuring accuracy.

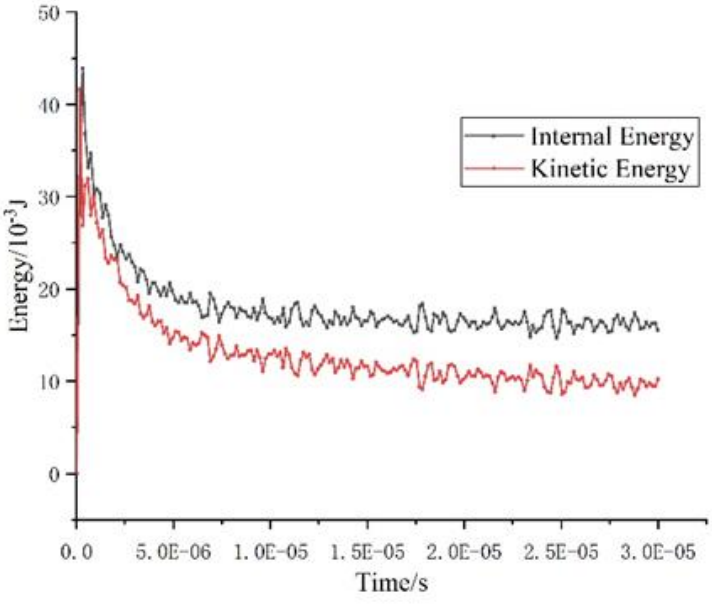

Figure 2.8- Single point impact energy curve

Conclusion to the Part 2

In this chapter, the numerical simulation of TB6 titanium alloy by laser shock peening is studied. A combination method of "Explicit dynamic + Implicit static" solver is adopted, which is suitable for multi-point impact reinforcement. Analyzed advantages and disadvantages of the *Elastic Perfectly Plastic* model, the *Zerilli-Armstrong* model, the *Johnson-Cook* model and the *Cowper-Symonds* model. The constitutive model of *J-C* material and related parameters of TB6 titanium alloy were determined. The geometric dimension of the model was determined, and the model was simplified under the condition that it met the experimental requirements and did not affect the stress results. Based on Fabbro's empirical formula and TB6 material properties, the optimal laser power density and energy range are 4.8~7.6GW/cm^2. That is meaning the energy range of laser is 6.8~10.8J. After analyzing the mesh convergence of the single point enhancement of the simple model, the mesh size of the local refinement area was determined to be 100μm. The grid size of the rest is 200μm. Finally, the energy change curve of the material in the strengthening process is analyzed, and the solution time of the Explicit analysis step is determined to be 1500ns. The above provides a strong basis for the numerical simulation of laser shock strengthening in the following chapters to study the optimal process parameters.

PART 3
ANALYSIS OF NUMERICAL SIMULATION RESULETS OF LASER SHOCK PEENING

Laser shock peening is a complex process, there are many factors that affect the result of effects, which can be mainly divided into two categories, one is the influence of different laser parameters, the other is the influence of different workpiece parameters. This chapter will mainly simulate and analyze the single laser shock peened hole circumference as well as hole wall with different laser parameters, and the laser shock peening of different spot overlap. Finally obtain the influence law of various factors on the strengthening results.

According to different impact areas, the local mesh refinement of different areas is adopted for the model, as shown in Figure 3.1. The size of the encrypted mesh is 0.1mm, and the element type is C3D8R. There are 2.2 million mesh on the hole circumference model and 1.7 million mesh on the hole wall model. In Figure 3.2, path 1 is the extraction path of residual stress when peening the hole circumference, and path 2 is the extraction path of residual stress when peening the hole wall. This simulation of laser shock peening process is to add pressure loading performance on the processing surface. The spot diameter is 3mm, and the single loading time is 60ns. Because the shock wave acts on the surface of the workpiece, the internal stress wave will be generated. In order to make the stress wave spread throughout the whole workpiece, the propagation time is set to 9940ns, and the total action time is 10^{-5}s.

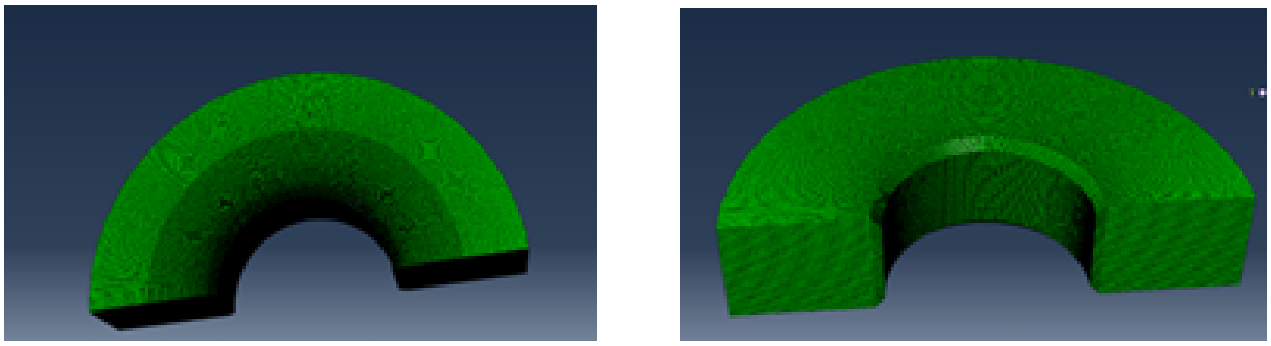

(a) Mesh refinement of hole circumference (b) Mesh refinement of hole wall

Figure 3.1 - Mesh refinement

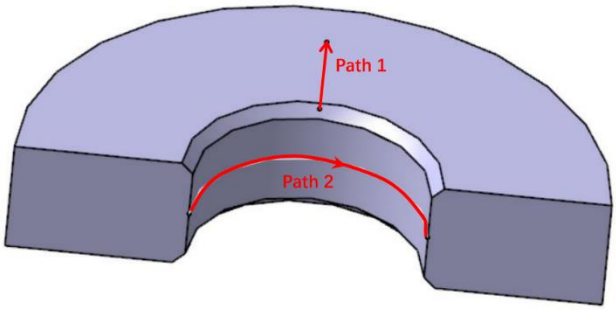

Figure 3.2 - The path of residual stress extraction

3.1 Single point laser shock peened hole circumference

3.1.1 Influence of power density on residual stress of hole circumference

According to the calculation in section 2.4, the optimal power density range is 4.8~7.6GW/cm^2. In order to make the result more rigorous, the power density range is increased to 4.8~8.8GW/cm^2. In this paper, numerical simulation is carried out at an interval of 1 GW/cm^2. The distribution of residual stress S_{22} on path 1 is shown in Figure 3.3. The depth of residual compressive stress extracted from the center point of the spot on the impact surface is shown in Figure 3.4. Residual stress fields under different power density are shown in Figure 3.5.

It can be seen from Figure 3.3 that with the increase of power density, the residual compressive stress around the hole is 460Mpa, 530 MPa, 560 MPa, 580 MPa and 560 MPa respectively. In the optimal range, the residual compressive stress increases with the increase of power density, but the increase amplitude decreases with the increase of power density. Once it exceeds 2.5 times the dynamic elastic limit of metal, the residual compressive stress does not increase but decreases. The influence depth of residual compressive stress will increase with the increase of power density, which are 0.35mm, 0.39mm, 0.60mm, 0.65mm and 0.67mm respectively. When the power density is 8.8 GW/cm^2, the depth of the influence layer is the deepest. Although the residual compressive stress of nearly 600MPa can be generated when the power density is greater than 6.8 GW/cm^2, the residual tensile stress of nearly 100MPa can also be generated, which greatly

affects the service life. Through the above analysis, the optimal power density for hole circumference strengthening is 5.8 GW/cm^2.

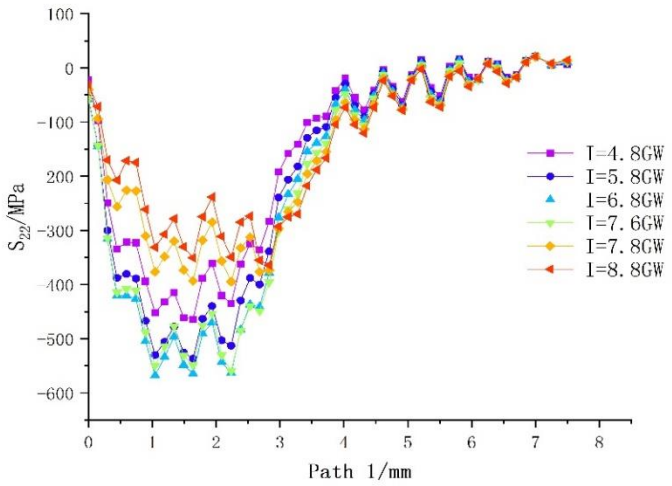

Figure 3.3 - Residual stress curve of hole circumference under different power density

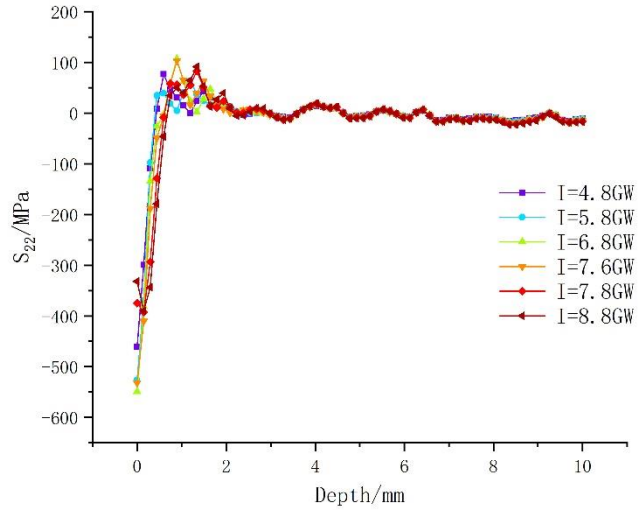

Figure 3.4 - Depth of residual stress layer in hole circumference under different power density

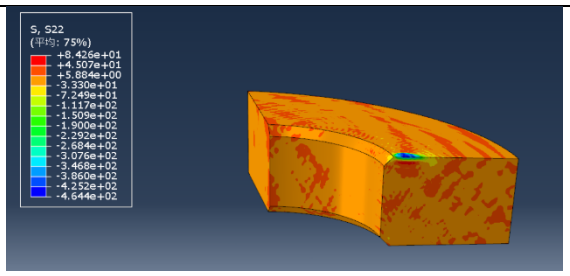

(a) 4.8 GW/cm^2

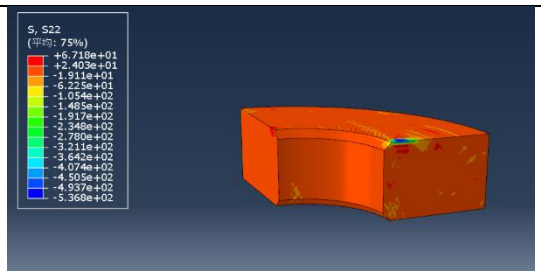

(a) 5.8 GW/cm^2

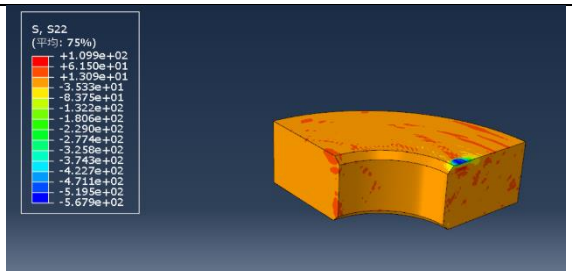

(c) 6.8 GW/cm^2

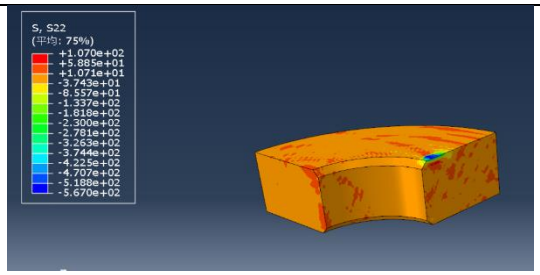

(d) 7.6 GW/cm^2

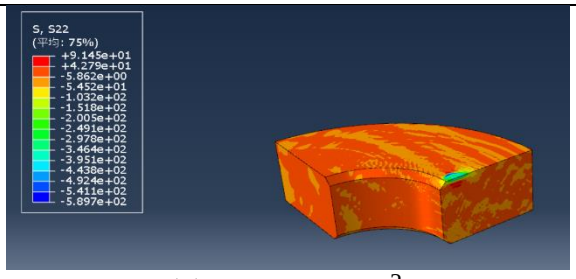

(e) 7.8 GW/cm^2

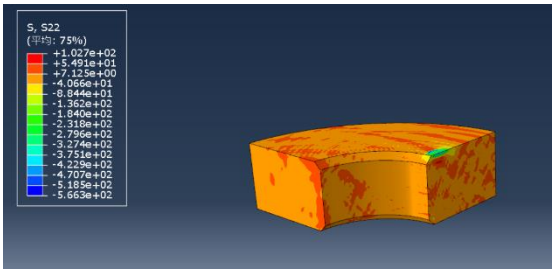

(f) 8.8 GW/cm^2

Figure 3.5 - Residual stress fields of hole circumference under different power density

3.1.2 Influence of impact times on residual stress of hole circumference

Multiple impacts can improve the distribution of residual compressive stress on the surface of machined parts and increase the influence depth of surface residual compressive stress and residual compressive stress. However, too many impacts increase the hardening dynamic yield strength of materials and weaken the plastic deformation ability of materials, making it difficult to achieve the strengthening effect. After three impacts, the residual stress on the surface of most metal materials will tend to be saturated, so the number of impacts is selected within 3. Select the laser with power density of 5.8 GW/cm^2, impact the surface of hole circumference for 1~3 times, and the loading time is a multiple of the times to analyze the distribution of residual stress field and the depth of action layer.

It can be seen from Figure 3.6 that with the increase of impact times, the residual compressive stress on path 1 around the hole is 560MPa, 680MPa and 740MPa respectively. After repeated impact, the surface grain of the material is refined, and the growth range of residual compressive stress is limited. It can be seen from Figure 3.7 that the depth of residual compressive stress layer is 0.60mm, 0.62mm and 0.70mm respectively. Although three times of impact can produce good residual compressive stress and layer depth, it brings

120MPa residual tensile stress. It can be concluded that the number of impacts on the area around the hole should not exceed 2 times.

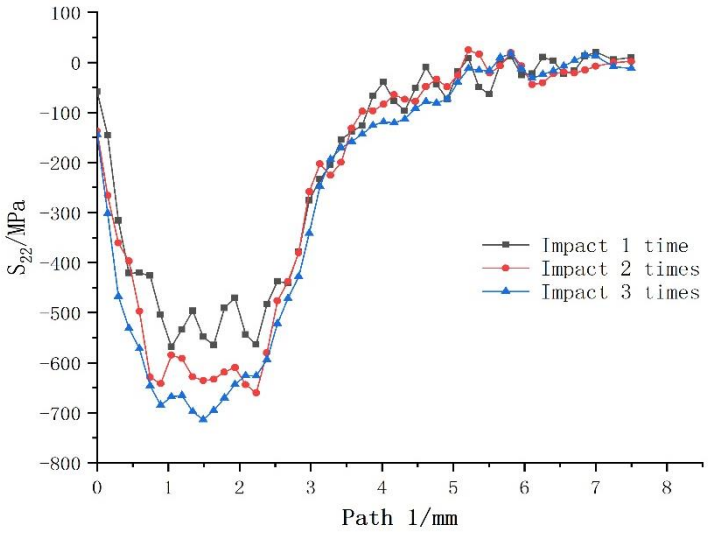

Figure 3.6 - Residual stress curve of hole circumference under different impact times

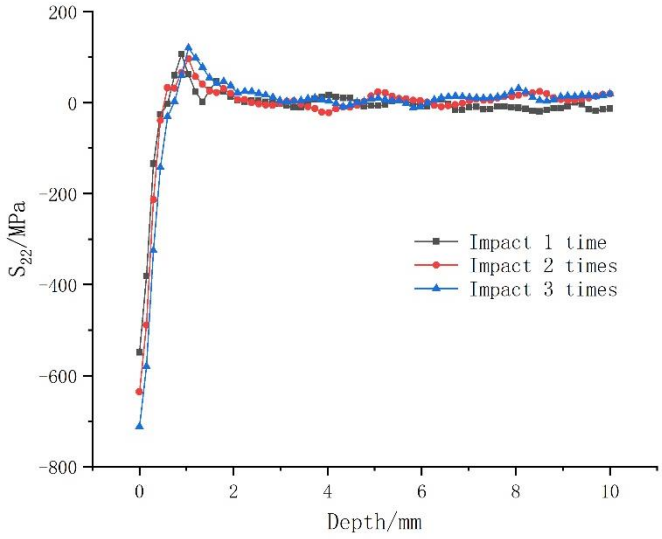

Figure 3.7 - Residual stress layer depth of hole circumference under different impact times

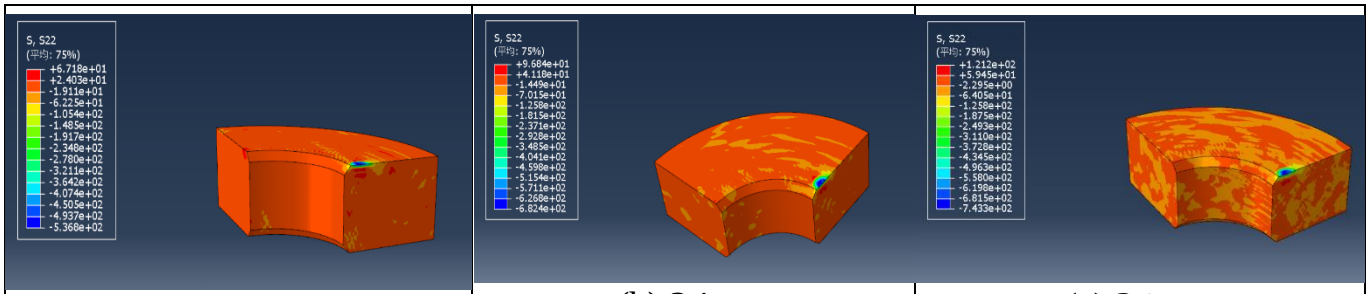

(a) 1time | (b) 2times | (c) 3times

Figure 3.8 - Residual stress fields of hole circumference under different impact times

3.2 Single point laser shock peened hole wall

3.2.1 Influence of power density on residual stress of hole wall

Similarly, the hole wall is impacted and strengthened by the laser power density at an interval of 1GW/cm^2. The distribution of residual compressive stress on path 2 is shown in Figure 3.9. The internal residual stress field is extracted from the center point of the light spot on the hole wall, as shown in Figure 3.10.

It can be seen from Figure 3.9 that with the increase of power density, the residual compressive stress on the hole wall is 470MPa, 580 MPa, 620 MPa, 610 MPa and 620 MPa respectively. When the power density reaches 6.8 GW/cm^2, the residual compressive stress on the hole wall is almost saturated and will not increase with the increase of power density. At the same power density, compared with the plane, the residual compressive stress on the concave plane such as the hole wall will be greater. The depth of residual compressive stress is 0.45mm, 0.51mm, 0.57mm, 0.72mm and 0.73mm respectively, and the power density exceeds 7.8GW/cm^2. The maximum residual compressive stress is generated at the surface below 0.14mm, that is, the surface. This is because the plastic deformation of the metal is saturated within a certain depth, and the power density continues to increase. The residual compressive stress on the surface decreases due to the enhanced plastic unloading effect of the reverse sparse wave, but in the area below the plastic deformation saturation zone, With the increase of power density, the plastic propagation is deeper, which makes the deeper material plastic deformation. It can be concluded that the optimal power density for hole wall strengthening is 6.8GW/cm^2.

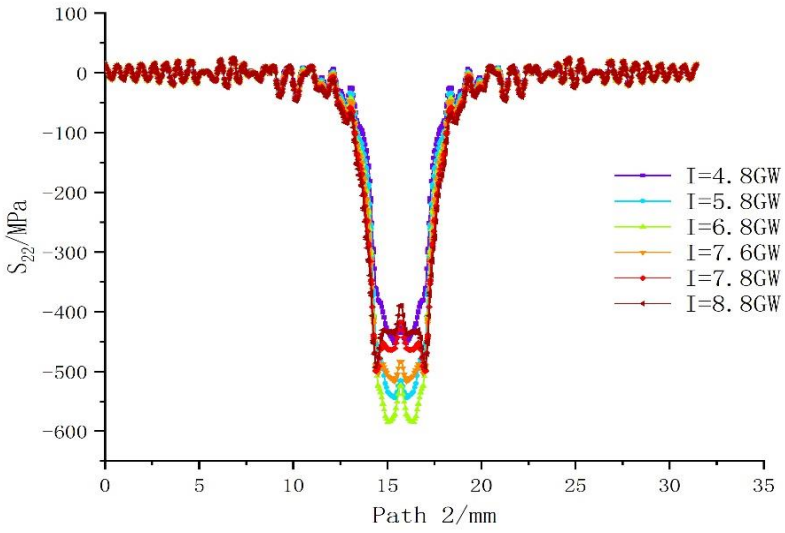

Figure 3.9 - Residual stress curve of hole wall under different power density

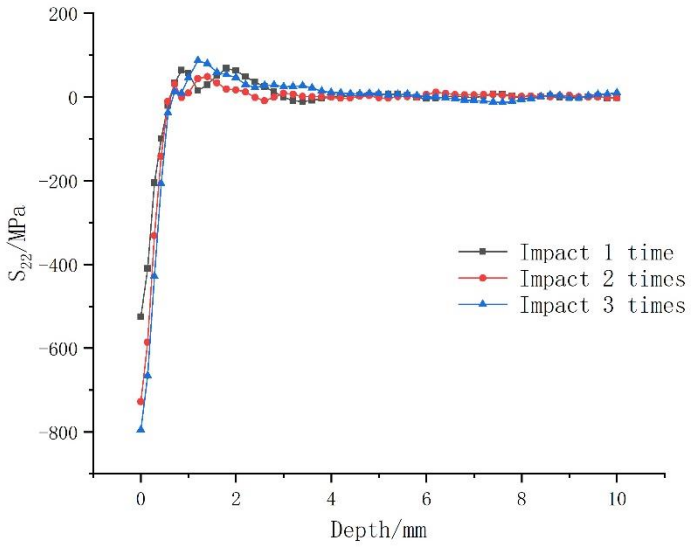

Figure 3.10 - Depth of residual stress layer in hole circumference under different power density

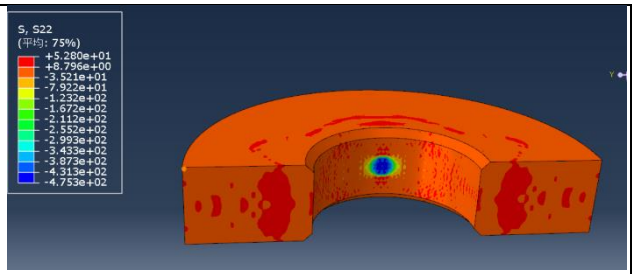

(a) 4.8 GW/cm^2

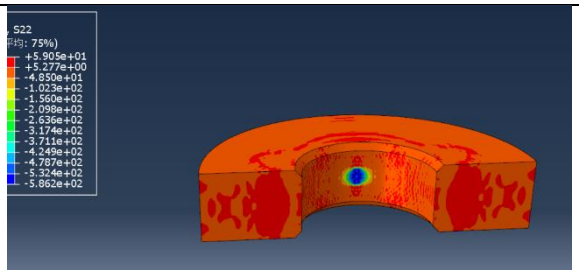

(a) 5.8 GW/cm^2

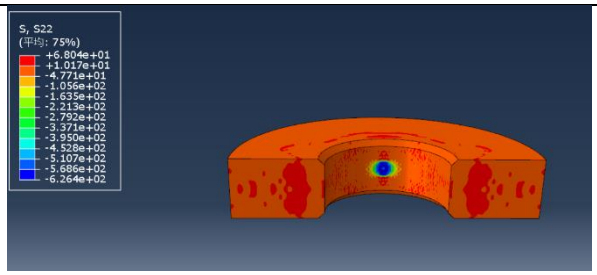

(c) 6.8 GW/cm^2

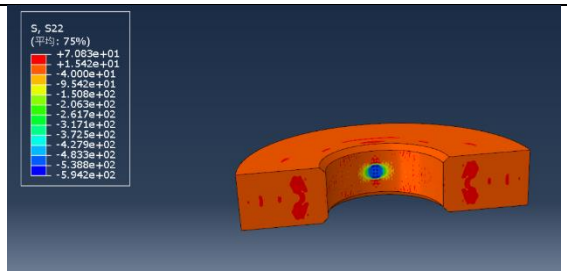

(d) 7.6 GW/cm^2

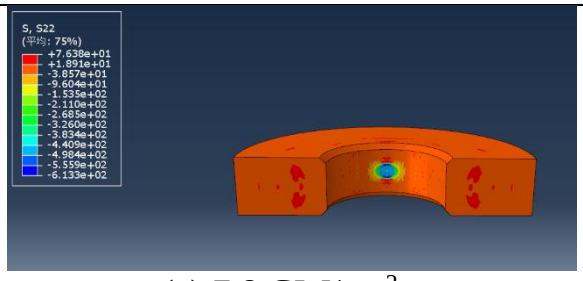

(e) 7.8 GW/cm^2

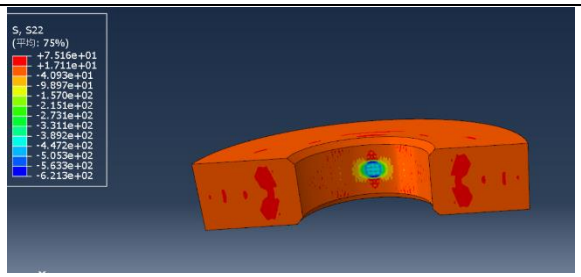

(f) 8.8 GW/cm^2

Figure 3.11 - Residual stress fields of hole wall under different power density

3.2.2 Influence of impact times on residual stress of hole wall

According to Section 3.2.1 of this paper, the impacted power density of the hole wall is optimized to be 6.8 GW/cm^2. Impact the hole wall surface for 1~3 times, and the action time of the shock wave is doubled in turn. Figure 3.12 shows the distribution of stress S_{22} measured along path 2, and Figure 3.13 shows the distribution of S_{22} at the central point of the impact spot.

It can be seen from Figure 3.12 that with the increase of impact times, the residual compressive stress produced by the hole wall of the test piece is 620MPa, 750MPa and 810MPa respectively, and the residual compressive stress produced by multiple impact on the hole wall surface is greater than that produced by the impact hole peripheral surface. It can be seen from Figure 3.13 that the influence depth of residual compressive stress on the hole wall is 0.57mm, 0.64mm and 0.68mm respectively. After three times of impact on the hole wall, the residual compressive stress can reach 810MPa, but the residual tensile stress can be well controlled within 100MPa, which not only ensures the impact effect, but also suppresses the adverse effects brought by multiple impacts. It can be concluded that the optimal impact times for the hole wall is 3 times.

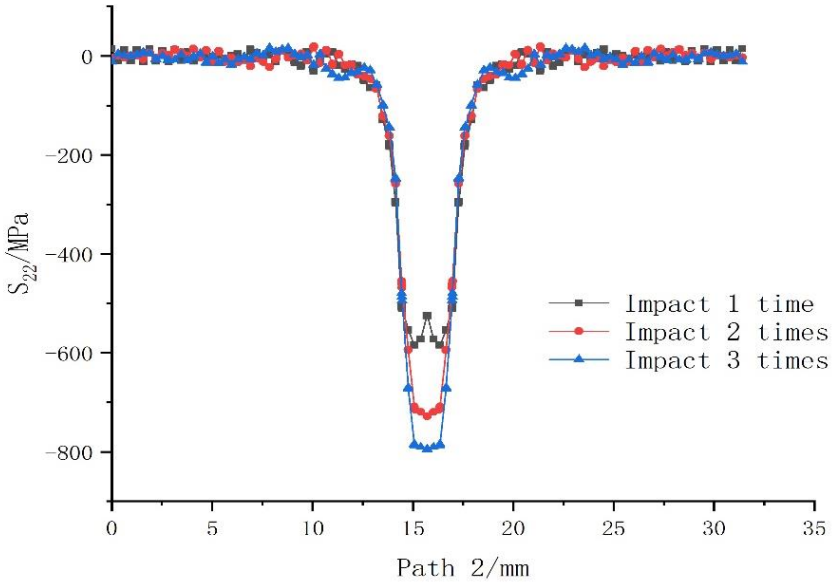

Figure 3.12 - Residual stress curve of hole wall under different impact times

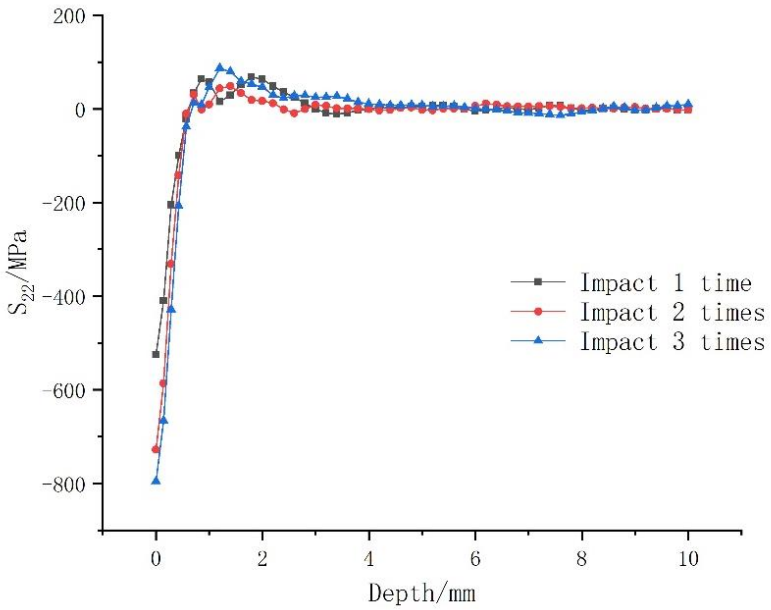

Figure 3.13 - Residual stress layer depth of hole wall under different impact times

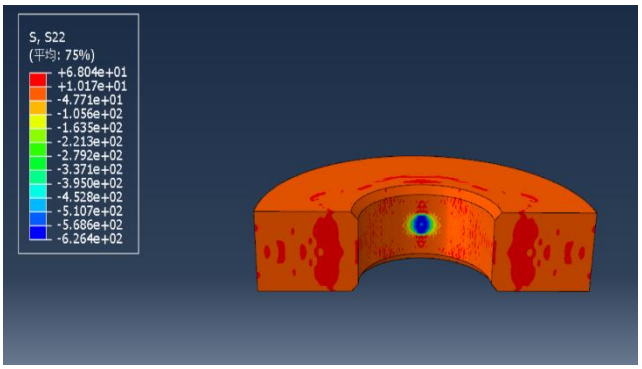

(a) 1time

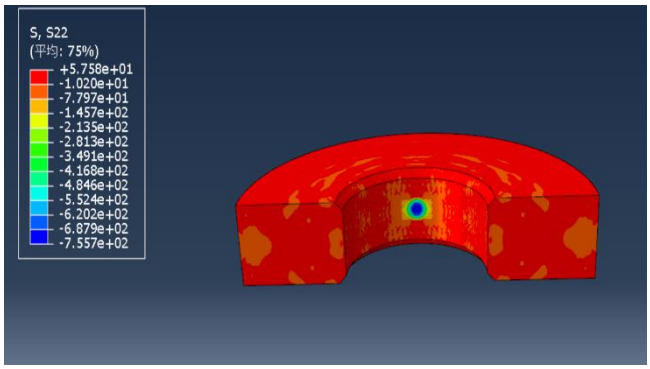

(b) 2times

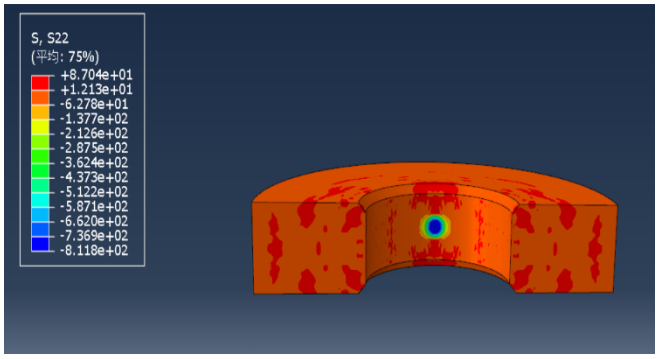

(c) 3times

Figure 3.14 - Residual stress fields of hole wall under different impact times

3.3 Multi-point laser shock peened hole

3.3.1 Influence of spot overlap rate on residual stress of hole circumference

In actual production and processing, single point impact generally cannot meet the needs of overall structural parts strengthening, so continuous laser shock peening is needed. Laser spots overlap rate is an important parameter in continuous laser shock peening. Selecting a reasonable laser spot overlap rate can quickly obtain high quality reinforced structural parts. The laser spot overlap rate η is calculated as follows:

$$\eta = \left(1 - \frac{L}{2R}\right) \times 100\% \tag{3.1}$$

In the equation 3.1, L - the distance between the center of two laser spots, R - the radius of the laser spot, in this paper the radius of laser spot is 1.5mm. If the overlap rate of laser spot is 0%, then L=2R; If η=25%, then L=3R/2; If η=50%, then L=R; If η=75%, L=R/2. Figure 3.15 shows the position distribution diagram of the spots when the diameter of the laser spot is 3mm and the overlap rate is 0%, 25%, 50% and 75% respectively. The distance between the adjacent spots is 3mm, 2.25mm, 1.5mm and 0.75mm respectively.

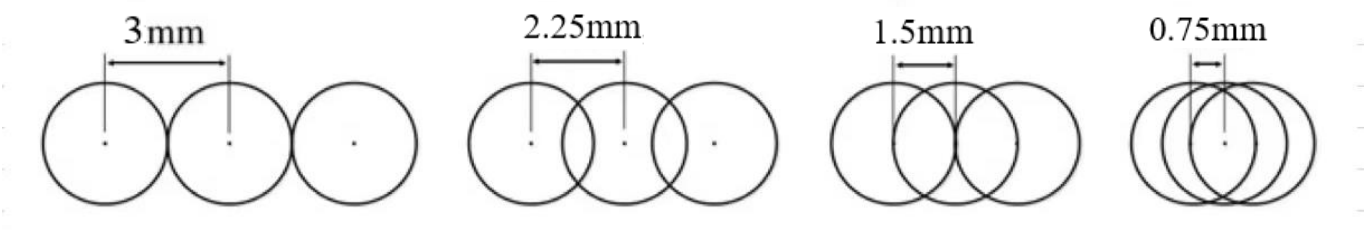

Figure 3.15 - Spot distribution when the spot overlap rate is 0%, 25%, 50% and 75%

In order to explore the influence of laser spot overlap rate on the strengthening effect, continuous impact the hole circumference was adopted. Figure 3.16 shows the cloud image of simulation calculation when the spot lap rate was 0%, 25%, 50% and 75%. As can be seen from the figure, the strengthening range decreases as the overlap rate increases. When the overlap rate is 0% and 25%, the distribution of residual compressive stress field is particularly uneven, and the stress difference between two points is large. When the spot overlap rate is 50% and 75%, there is no significant difference in stress between the spots. Therefore, in the multi-point laser shock peening of structural parts, selecting the

appropriate spot overlap rate can achieve a balance between the strengthening rate and strengthening effect, and obtain high quality strengthening results quickly.

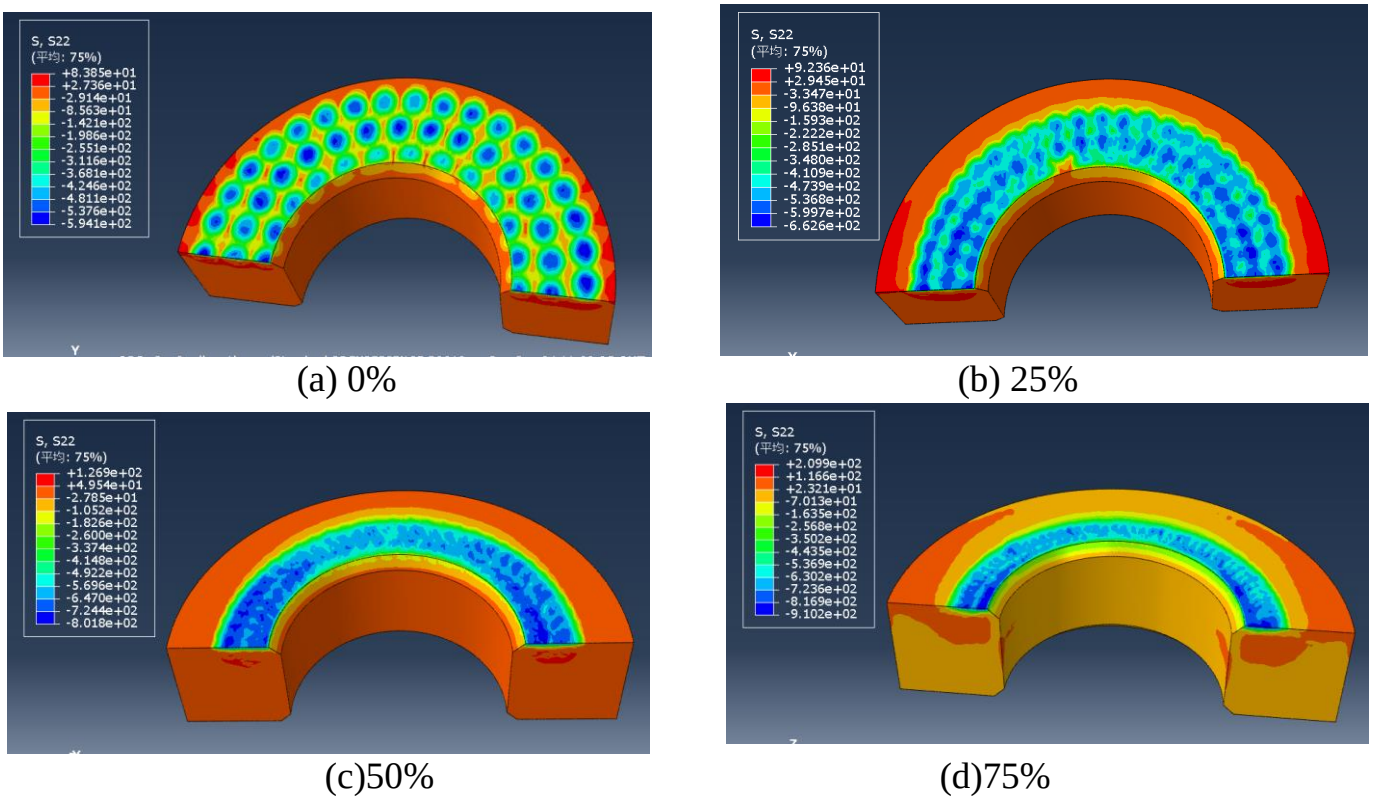

Figure 3.16 – Residual stress fields of hole circumference with different overlap rates

Figure 3.17 (a) shows the residual stress field curve of the shock surface and (b) shows the distribution curve of the deep residual stress at the origin of the impact center under different spot overlap rates. It can be seen from Figure 3.17 (a) that when the laser spot overlap rate is 0% and 25%, the residual stress curve of the strengthened surface shows obvious jump phenomenon and uneven distribution of the residual compressive stress. However, the surface residual stress distribution curve is relatively smooth when the spot overlap rate is 50% and 75%, and there is no obvious phenomenon of stress jumping. In the actual strengthening production, the peening time will be greatly extended after the increase of the overlap rate, and the 50% overlap rate has met the requirements of the strengthening quality. Therefore, the 50% overlap rate is generally used as the overlap rate used in production. As can be seen from Figure (b), when the overlap rate is 0% and 25%, the residual stress curve in the depth direction of the strengthening center is almost the same. When the overlap rate increases to 50%, the depth of the residual stress layer increases from

0.49mm of 25% to 0.68mm, and when the lap rate is 75%, the depth of the residual compressive stress layer increases to 0.97mm. Therefore, with the increase of spot overlap rate, the depth of residual stress layer also increases gradually. When the lap rate is 50%, the maximum residual compressive stress at the center is significantly increased compared with 0% and 25%, and the average compressive residual stress can reach 651MPa, which is increased by 200MPa. When the lap rate is 75%, the average compressive residual stress fluctuates around 725MPa, and the increase rate is significantly slowed down. The main reasons for the above two points are as follows: with the increase of spot overlap rate, the area of repeated strengthening on each spot increases, which is equivalent to two or even three shocks on the basis of single point strengthening, and this phenomenon becomes more obvious with the increase of spot lap rate. Therefore, the increase of spot lap rate will lead to the increase of maximum compressive residual stress and the depth of compressive residual stress layer.

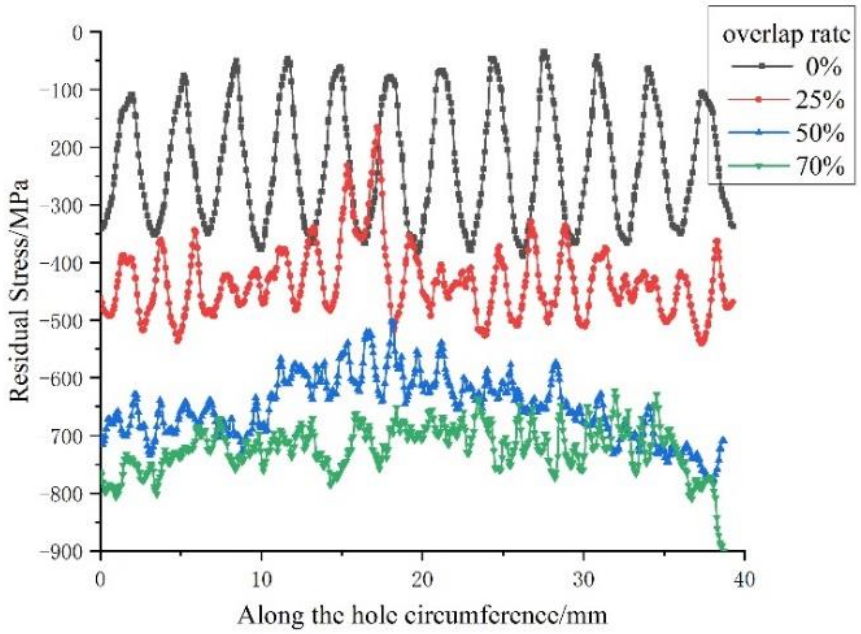

(a) Residual stress field curve of the shock surface

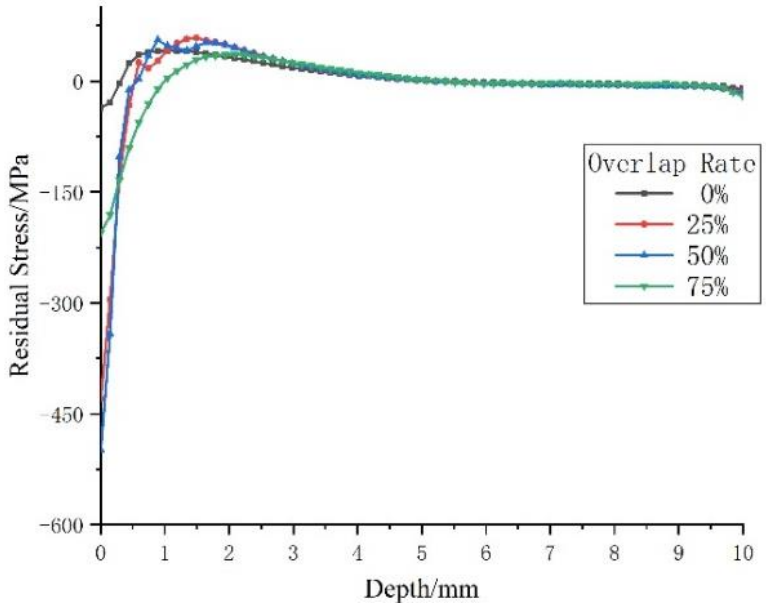

(b) Residual stress layer depth curve of the shock surface

Figure - 3.17 Residual stress distribution of hole circumference curves under different spot overlap rates

3.3.2 Influence of spot overlap rate on residual stress of hole wall

Figure 3.18 shows the residual stress field curves of hole walls at different lap rates. As can be seen from Figure 3.18(a), when the lap rate is 0%, the residual stress between the two spots is excessive and uneven, resulting in a stress difference of 500MPa. When the overlap rate is 25%, the stress difference between two adjacent spots decreases to 200MPa, and the maximum compressive residual stress can reach 726MPa. When the overlap rate is 50%, the maximum compressive residual stress is 732MPa, and the residual compressive stress at each point fluctuates around 700MPa, and the stress difference between two points decreases to 75MPa, indicating a stable stress field. When the lap rate is 75% and the maximum compressive residual stress reaches 766MPa, the effect is not much improved compared with that when the lap rate is 50%, and the maximum stress difference between each point is 100MPa. Figure 3.18(b) shows the stress layer depth curves at different lap rates. When the lap rates are 0%, 25%, 50% and 75%, the maximum stress layer depth is 0.46mm, 0.50mm, 0.64mm and 0.65mm. The reason for this phenomenon is that the hole wall, as a concave plane, can generate a larger and deeper residual stress layer under the same impact pressure, but the material surface will be work-hardened under a small shock pressure, which also explains that when the overlap rate reaches more than 50%, the residual

stress field does not change significantly and the layer depth cannot be further deepened. Therefore, the best overlap rate should not exceed 50% when machining hole wall, which can not only improve the processing efficiency, but also ensure the processing effect.

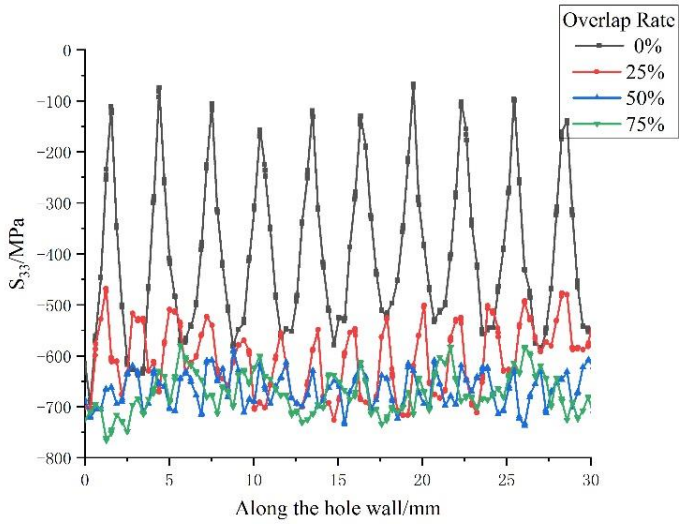

(a) Residual stress field curve of the hole wall surface

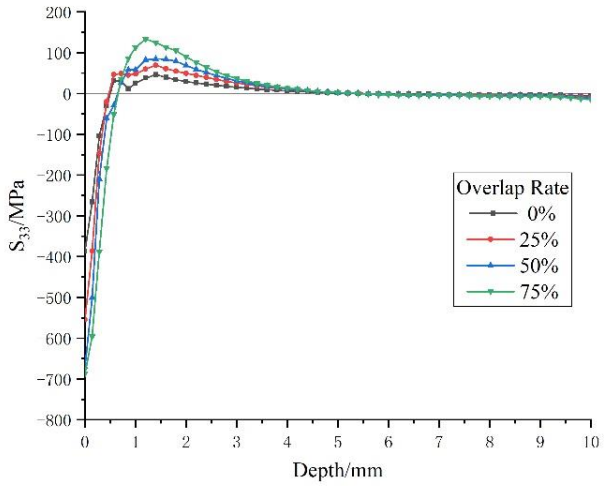

(b) Residual stress layer depth curve of the hole wall surface

Figure - 3.18 Residual stress distribution of hole wall curves under different spot overlap rates

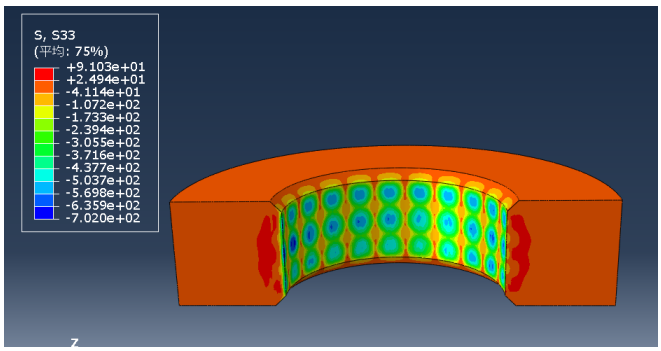

(a) 0%

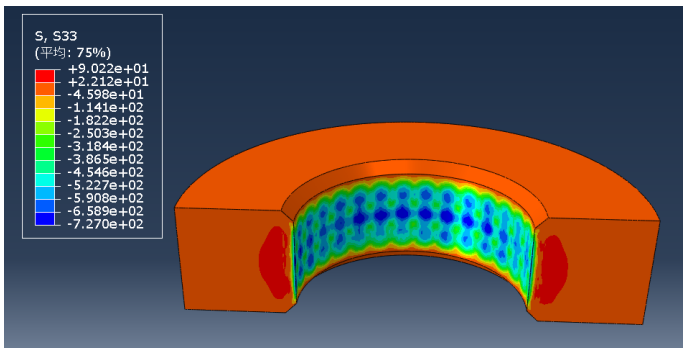

(b) 25%

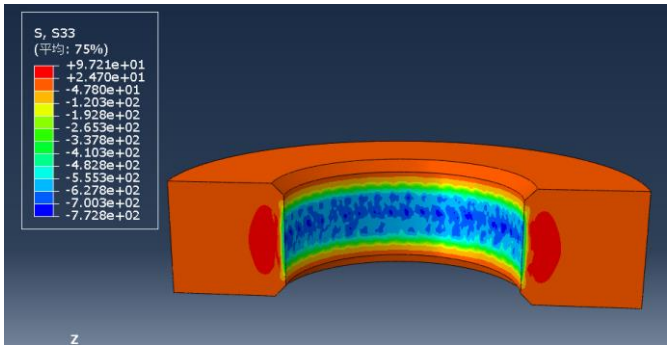

(c) 50%

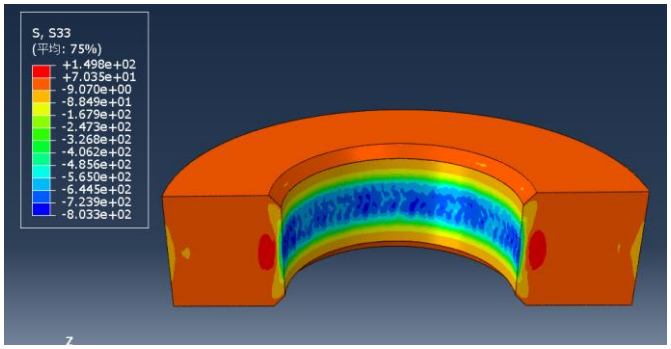

(d) 75%

Figure 3.19 – Residual stress fields of hole wall with different overlap rates

Conclusion to the Part 3

There are many factors affecting the result of laser shock peening. In this chapter, the finite element simulation method is used to simulate TB6 material as the impact object. The influencing factors of single point laser impact peening were analyzed, and the influence laws of power density and impact times on the results of single point laser impact peening were summarized as follows: 1) When the power density is 5.8 GW/cm^2, 530MPa residual compressive stress is generated in the area around the hole, affecting the layer depth of 0.39mm; Compared with the hole circumference surface the single point impact hole, the residual compressive stress generated on the impact hole wall surface is larger and the strengthening effect is better. When the power density is 6.8 GW/cm^2, 620MPa residual compressive stress is generated in the hole wall area, affecting the layer depth of 0.57mm. 2) Increasing the impact times can increase the residual compressive stress and deepen the influence depth of residual compressive stress, but too many times will cause excessive residual tensile stress. Impact on the surface around the hole twice can produce 680MPa residual compressive stress, affecting the layer depth of 0.62mm; Impact on the hole wall surface for 3 times can produce 810MPa residual compressive stress, affecting the layer depth of 0.68mm.

The laser shock peening simulation with different spot overlap rates was carried out, and the effect law of laser spot lap rates on laser shock peening results was obtained as follows: For the circumference and wall of the hole, the residual stress field will be uneven when the bonding rate is below 50%, and the stress difference between two points is small and gentle when the bonding rate is above 50%, and the stress distribution is uniform.

PART 4
LABOUR PROTECTION

The principle of laser shock peening is that the laser beam generated by the laser irradiates on the surface of the absorption layer to generate plasma, and the plasma diffuses towards the target under the constraint of the constraint layer to form detonation waves, which impact on the surface of the machined parts. The intense laser emitted by the laser has a power density of up to $10^9 W/cm^2$, a plasma temperature of up to $10^7 K$, and a peak pressure of up to 1GPa. Therefore, when operating the laser shock peening related equipment, the operator should be careful to prevent the injury caused by the laser beam. The equipment for laser shock peening is usually operated by engineers, and is mainly responsible for the adjustment of process parameters for shocking parts. This chapter will discuss the working conditions of the laser shock peening laboratory and the precautions for the staff.

4.1 Harmful and hazardous working factors

This section will discuss the safety and health problems that may occur during the laser shock peening process, which is related to the health of workers in the work process and the impact of the working environment on the work process.

According to GOST 12.0.003-2015, the dangerous and harmful factors that may be encountered when manipulating laser shock peening equipment includes:

- The part clamping robot moves without control;
- Direct, reflected, and diffused light produced by lasers;
- Smoke and steam generated by laser ablation on the surface of the absorbing layer;
- High voltage circuit electrocution

The clamping robot is responsible for moving the clamping part according to the specified route to achieve multi-point impact, as shown in Figure 4.1. A robot arm usually weighs up to 500 kg, which is too heavy for an average adult man to support. When the movement of the robot arm is uncontrolled, it will cause untold mechanical damage and possibly death to those near the robot arm.

Figure 4.1 – Clamping robot arm of laser shock peening

The most obvious harm is the possibility of blindness. Even if the laser wavelength used is outside the eye's sensitive range (400-1400nm, visible and near infrared light), it can still cause eye damage. Although there is no longer any need to worry about direct laser blindness outside the sensitive range, there are still many other ways to expose your eyes to laser energy damage. Eye burns, distorted eye shape, reduced vision, boiling eye fluid, degeneration (decay) of proteins in the eye leading to milky blind spots and internal bleeding are all possible symptoms of laser input directly into the eye. Likewise, the mere fact that the beam is not visible light (400-700nm) or near-infrared light (700-1400nm) does not prevent instantaneous damage and blinding. If the laser's energy output is high enough, it can still cause immediate burns, like touching a hot stove top. In addition, for direct exposure to the laser, indirect exposure of the reflected beam can also be dangerous, depending on the situation. There are two types of reflection: specular reflection (where a

beam of light is reflected or partially reflected from a smooth surface or through the glass, where the beam continues on its new path) and diffuse reflection (where light scatters in all directions from a rough surface such as glass). When the beam is reflected, some of the energy is partially dispersed, but if the laser has enough initial energy, the reflected beam can still be dangerous. Because the reflected beam is still coherent with the laser, it should be treated the same as a beam coming directly from the laser source. Diffuse lasers are usually dispersed enough to make them harmless, but the diffuse light from Class 4 lasers is powerful enough to be irritating to the eyes, and vision can deteriorate over time if the eyes are not properly protected.

Smoke and steam hazards are similar to welding hazards and require high temperature operating safety specifications -- many industrial lasers are used for cutting, etching, and ablative (e.g., sanding or grinding) to burn off materials. This gives high power lasers the same hazards as many high-temperature operations such as welding. According to the law of conservation of mass, burned materials do not disappear and disillusionment. When these substances are burned, some of them will exist in the air as toxic gases. Laser combustion of metals and other solid materials as well as oils, solvents and other chemicals produces toxic exhaust gases that burn and melt into or evaporate into the air when exposed to the concentrated energy of the laser.

The laser emitter needs a powerful voltage to start. When the circuit is aging or the copper wire is exposed due to rodents chewing on the wire skin, it is particularly easy to cause short circuit of the wire and the risk of electric shock.

4.2 Analysis of working conditions and development of protective measures

In order to mitigate the above hazards, the laser shock strengthening equipment is provided with a screen door. The laser and the clamping robot are placed in a ventilated environment isolated from personnel, and the machine must be started without any personnel inside the screen door. Wear goggles with the corresponding wavelength during the whole process of laser shock intensification to avoid laser leakage. In addition, the following precautions need to be strictly implemented to avoid unnecessary hazards.

1. Some laser work will emit infrared, ultraviolet light invisible to the human eye, do not think that the laser failure and to check with the eye, when checking the laser must ensure that the laser in the case of power off.

2. If the laser may stop working due to a fault or power failure, confirm that the laser is powered off before performing the check.

3. Even if you wear a laser protection mirror, you can not look directly at the laser emission port.

4. Do not look directly at the reflected light of laser above Class IV (>500mW). Please wear a laser protection mirror when using this kind of laser.

5. It is forbidden to place inflammable and explosive articles and black paper, cloth, leather and other materials with low ignition point on the laser path (except laser damage experiment).

6. The laser above Class IIIa (5mW) may cause burns to the human body. Do not direct the laser at the human body.

7, do not place the laser in the place where non-professionals can reach.

8. Do not direct the laser at the glass in front of you. Conventional glass has a reflectivity of about 4%, which can cause damage from laser light that bounces back into the eye.

9. When you build the experimental platform, there will be a "working plane" at the height of the laser emission port. Do not put your head close to this working plane during laser work, because the light reflected and transmitted by the lens and mirror group may enter the eyes and cause damage. Do not lift the laser emitting port and mirror; otherwise, the laser may enter your eyes and cause damage.

10, when you use the laser work, please remove your watch, to avoid the watch reflected light into the eye to cause injury.

11. When using infrared lasers, lasers with wavelengths greater than 800nm are almost completely invisible. Please use a detector or up - converter to determine the position of the laser.

12. Please note that the visual intensity of some laser bands (such as those with wavelengths lower than 430nm or higher than 700nm) is significantly weaker than the actual intensity.

13. The peak power of pulsed (Q-switched, mode-locked, ultra-fast) laser is very high, which may cause damage to the experimental components. Please confirm the anti-damage threshold of your test pieces before use.

14. Please place a black metal plate at the end of the experimental environment to prevent the laser from leaking into the space outside the work area.

Recommendations for laser use:

- when you use laser, we strongly recommend that you wear the corresponding wavelength of laser protection goggles, in order to protect your eyes from the threat of laser.

- We suggest that you wear long white clothes, so that even if the laser shines on the body, it will not burn your clothes and cause a fire.

- When using UV laser, we recommend that you apply sunscreen with SPF30 or above on the surface of your exposed skin to protect your skin from UV light.

4.3 Fire Safety Rules at the workspace

Measures to be considered in accordance with DBN A.3.2-2-2009 requirements for fire prevention and protection, and in accordance with DSTU 7113:2009 requirements for explosive environments. Fire and explosion safety refers to a state that excludes the possibility of fire and explosion of objects and prevents the action of fire and explosion risk factors on people in the case of fire and explosion.

Laboratories using plasma generators have fire safety Class D. Although indoor hazards are low, electrical currents can cause fires due to damaged insulation, poor wiring, or short circuits. In order to avoid dangerous situations, the electrical equipment is equipped with automatic overload protection and short circuit protection. The room is also equipped with a dry powder fire extinguisher. Powder fire extinguishers OP-1, OP-25, OP-10 are used to extinguish small fires of flammable liquids, gases, electrical installations with voltage up to 1000V, metals and their alloys.

The room is also equipped with a fire alarm. To do this, install a smoke alarm sensor in the ceiling.

Conclusion to the Part 4

In this part, the hazards that engineers are prone to suffer in the process of laser shock strengthening due to working process factors and environmental factors are comprehensively considered, mainly including the damage to eyes and skin caused by laser irradiation, the damage to respiratory tract caused by vaporized substances, the damage to high-voltage electrical contacts and the mechanical damage to people caused by mechanical arm movement.

In combination with relevant laws and regulations, in order to avoid the above hazards, some targeted measures and precautions have been put forward. Such as safety doors are set between equipment and people, and people must ensure that the power supply of equipment is stopped during maintenance. During the whole process, they must wear protective glasses, and if possible, they can wear long white clothes and masks to protect themselves. And so on.

It is hoped that a series of measures can effectively mitigate the probability of safety accidents and reduce unnecessary casualties and property losses. The placement of fire protection facilities shall meet the current national standards of Ukraine.

PART 5
ENVIRONMENTAL PROTECTION

5.1 Pollution in machining field

Due to the lack of environmental protection concept, many employees of small mechanical processing enterprises are generally in debt in the construction of environmental protection facilities, resulting in many environmental problems. The main types and characteristics of pollutants are as follows: cutting dust, polishing and polishing dust, welding smoke, etc. of toxic and harmful substances will be generated during the production process of mechanical processing. Long term work and life in such an environment will endanger your health.

In addition, a large number of solid wastes such as metal scraps, scrap metal chips and welding slag, which are not treated for a long time and are scattered in the open air, will also pollute the surrounding environment. There are also various types of oily cotton yarn and oily gloves that can also pollute the surrounding environment if they are not handled properly.

Liquid substances commonly used in machining process, such as cutting fluid and lubricating oil, will become serious pollutants and endanger people's health if they are not handled properly in use. The cutting fluid is often used in the cutting process, which contains hydrocarbons, formaldehyde, sodium nitrite and other substances that pollute the water environment. The workers are often exposed to these substances during the processing process, which will endanger their health. The lubricating oil is yellow viscous liquid, which is flammable. It is flammable in case of open fire and high heat. If the skin is not cleaned in time, it may cause dermatitis and pimples in minor cases, dermatitis or skin tumors in severe cases, accidental entry into the mouth or inhalation into the body, gastrointestinal disease or pneumonia in minor cases, and cancer in severe cases. If the waste cutting fluid and lubricating oil produced in the processing process are not properly treated, they will become serious pollution sources.

The waste gas produced in the production process of the mechanical processing industry, which is harmful to the environment, includes painting waste gas, heat treatment

waste gas, etc. It contains volatile organic compounds. If it is simply treated, it will cause serious environmental problems.

Exhaust gas pollution source is dust, welding fume or paint exhaust gas, etc; The dust generated in blanking, cutting, grinding and other processes, as well as the welding smoke generated in the welding process, are generally discharged out of the plant through unorganized emission. Many small machining enterprises have backward painting waste gas treatment process, which cannot meet the emission standards; There are even outdoor paint spraying, and the paint exhaust gas is directly discharged in an unorganized form without collection and treatment measures.

The noise pollution source is mainly the noise generated by the operation of various equipment during production and processing, such as punch, plate shear, grinder, lathe, etc.; At present, the measures taken include plant sound insulation and distance attenuation.

5.2 Pollution prevention measures

The first is to establish a long-term inspection and supervision mechanism. Strict environmental assessment of enterprise project construction is the most basic guarantee, and environmental protection facilities must be built as required for project construction, so that qualified production can be guaranteed. However, due to the weak awareness of environmental protection of some operators, even if environmental protection facilities are built, they are not used in normal production, but only used as props to cope with inspection. Therefore, these facilities are often just decorations. This situation leads to prominent environmental pollution problems in the production process, and the environmental pollution problems of enterprises that organize production without passing the environmental assessment are even more obvious. Therefore, it is very necessary to establish a long-term inspection and supervision mechanism, which will ring the alarm bell for those opportunistic operators all the time, reminding producers that they must organize production according to environmental requirements, otherwise, the corresponding punishment measures will make them unable to continue production. At the same time, it also sends a positive signal: only by organizing production according to environmental requirements, can enterprise production develop healthily.

The second is to strengthen the continuing education of employees, so that they can understand the impact of the production process on the environment and the harm it brings, at the same time, through the study of relevant laws to make them understand their responsibilities, improve and strengthen the environmental awareness of employees, especially business operators, and in combination with the establishment of a long-term inspection and supervision mechanism, cultivate the environmental awareness of business operators, so that environmental protection becomes their conscious behavior.

Third, in accordance with relevant laws and regulations, further improve the construction of storage sites for general solid wastes and hazardous wastes, standardize the storage and treatment procedures for various hazardous wastes, and establish accounts and archives for hazardous wastes; Smooth handling and strict supervision responsibility.

The fourth is to put forward the following suggestions on the specific problems: the leakage pollution of grinding fluid and waste lubricating oil should be said to be the most common problem. New processes - low pollution micro lubrication and the use of environment-friendly transparent microemulsion grinding fluid can be used to reduce the generation of pollutants from the source and reduce their harm to the ecological environment and human health. Wang Canhui, et al. introduced a new environment-friendly transparent microemulsion grinding fluid, which does not contain sodium nitrite and other harmful elements. The test shows that the microemulsion grinding fluid has good rust resistance, lubricity and stability, and the product performance fully meets the requirements of relevant standards, and reduces environmental risks. Jia Dongzhou and others summarized and looked forward to the current situation of grinding cooling and lubrication, and mentioned the advantages of micro lubrication application. Micro lubrication uses biodegradable vegetable oil as the lubricating base oil, which can effectively reduce the cost of grinding fluid maintenance and post-treatment, and also avoid its harm to the environment and human health.

In view of the leakage pollution of grinding fluid and waste lubricating oil, in combination with the layout adjustment of the plant area, the ground in the processing machinery placement area can be anti-seepage treated, and diversion ditches are set around to collect waste lubricating oil, grinding fluid, etc., for centralized treatment. If conditions

are not met, waste liquid trays can be attached to the ground below the leakage around the equipment to receive waste lubricating oil and grinding fluid, so as to prevent waste lubricating oil and grinding fluid from leaking to the ground. The pollution of waste paint and waste gas in paint spraying room is a prominent problem. Wang and others introduced two technologies of dry paint spraying room in view of the shortcomings of wet paint mist capture device, showing its benefits in the recycling of exhaust air and in energy conservation and environmental protection. Hu and others introduced the application of waste gas purification equipment in the existing painting production line and paint spraying

The feasibility scheme for treatment and transformation of indoor waste gas makes the project achieve the goal of reducing investment, reducing equipment operation cost and meeting the emission requirements of environmental protection policies as far as possible. Aiming at the problem of waste paint and waste gas pollution in the paint spraying room, combined with the rectification, the process facilities such as photocatalysis adsorption can be used to treat the paint waste gas, and the emission concentration of the waste gas can be monitored regularly, and the activated carbon can be replaced regularly to ensure that all kinds of waste gas generated in the production and operation process can be stably discharged up to the standard, and the source of the total amount of volatile organic pollutants can be determined.

The concept of environmental protection runs through the whole process of laser shock strengthening. In the selection of constraint layer materials, deionized water is the first choice to replace the organic glass. It is a huge waste to replace the organic glass every time it is impacted. The deionized water can be recycled in production after being filtered by the filter screen. There are two kinds of absorption layer materials: aluminum tape and black tape. Black tape is easier to obtain and has lower cost. Aluminum tape has high cost and is complex to manufacture. The gasification gas generated in the laser shock strengthening process will be absorbed by a special air filter screen, and then discharged into the atmosphere after non-toxic treatment.

Conclusion to the Part 5

Mechanical processing enterprises cause certain pollution to the environment in the process of mechanical processing. By strengthening the environmental protection awareness of employees, improving the environmental protection concept of employees, taking targeted environmental pollution control measures, and establishing a long-term inspection and supervision mechanism, the pollution of small mechanical processing enterprises to the regional environment can be effectively reduced. The environmental protection concept shall be implemented in the whole process of laser shock peening production activities.

GENERAL CONCLUSION

In this paper, ABAQUS finite element simulation software was used to establish a three-dimensional finite element model for laser shock peening of the hub hole structure of TB6 titanium alloy helicopter rotor. The effects of laser shock peening position, overlap rate, times of shocks and other process parameters on the residual stress field of the hole structure were studied. The numerical simulation results are as follows:

- In order to get accurate simulation results in a short time, the basic research of simulation is carried out. An efficient basic research model is established. The spatiotemporal distribution model of pressure wave is obtained which accords with the actual situation. Calculate the optimal laser energy range; Select accurate and efficient mesh size; The time length of dynamic analysis in simulation was obtained. It lays a foundation for the simulation research of the following paper.

- The effects of single point laser shock strengthening on the strengthening results under different process parameters were simulated and studied. Taking the residual stress as the judging index, the compressive residual stress can be improved by increasing the laser power density and the number of shocks during the single point impact strengthening. At the same time, attention should be paid to the influence of excessive residual tensile stress on material properties. When the plastic deformation of the material is saturated, it is of no use to increase the laser power density and the number of shocks. Under the same power density, the residual compressive stress increases obviously in the impact hole wall compared with the impact hole circumference. The optimal power density of single point impact hole wall is 6.8 GW/cm^2 which can bring 750MPa residual compressive stress and 0.64mm layer depth. The hole wall will produce 810 MPa residual compressive stress after 3 times laser shock peening, and the depth of residual compressive stress is 0.68 mm. The optimal power density of single point impact hole circumference is 6.8 GW/cm^2 which can bring 560 MPa residual compressive stress and 0.60mm layer depth. The hole circumference will produce 680 MPa residual compressive stress after 2 times laser shock peening, and the depth of residual compressive stress is 0.62 mm.

- Multi-point laser shock peening, in order to study the influence of improving spots lap rate on the residual stress field, the control variable method was adopted to keep the energy density of 6.8 GW/cm^2, the diameter of 3mm circular spot, the absorption layer is black tape, the constraint layer is deionized water and these parameters remained unchanged, and the spot lap rate was changed to 0%, 25%, 50%, 75%, respectively. The results show that the optimal overlap rate of both the hole wall and the hole circumference is 50%. When the overlap rate is 50%, the average residual compressive stress around the hole can reach 650 MPa and the stress depth is 0.68 mm; the average residual compressive stress on hole wall is 700 MPa, maximum residual compressive stress is 732MPa, and the stress depth is 0.64 mm.

Since the processing should be carried out by the engineer in the laser shock peening laboratory, the working conditions must meet the established standards for using lasers. In the part of labor protection, I reviewed the regulatory documents, listed the general harmful factors that engineers may be exposed to in the process of performing work tasks, and stipulated the operation specifications and accident handling procedures in the workplace. In terms of environmental protection, the possible pollution in the traditional machining field was investigated, the corresponding pollution treatment measures were taken, and the concept of environmental protection was introduced into the laser shock peening work.

REFERENCES

1. Manson S S. Metal fatigue damage [M]. 1976, 31-33.
2. Xu Bingshi, Ma Shinig, Liu Shishen, etc. Nano surface engineering [M]. Beijing, 2000. (in Chinese)
3. Li Jingui. Modern Surface Engineering Design [M]. Beijing, 2000. (in Chinese)
4. Liu Suo. Fatigue properties of metal materials and shot peening process [M]. Beijing,1997.
5. Prevey P S, Jayaraman N. Low plasticity burnishing treatment to mitigated fod and corrosion fatigue damage in 17-4 PH stainless steel[C]. Proceedings of the TriService Corrosion Conference. Lambda Research, 2003: 7-21.
6. C Rubio-Gonzalez, J L Ocan, G Gomez-Rosas, et al. Effect of laser shock processing on fatigue crack growth and fracture toughness of 6061-T6 aluminum alloy[J]. Materials Science and Engineering A, 2004, 386: 291~292.
7. A H Clauer, D F Lahrman. Laser shock processing as a surface enhancement process[J]. Key Engineering Materials, 2001, 197: 121~142
8. Wang Yanli, Zhu Youli, Cao Qiang, Zhang Xiaohui. Progress and prospect of research on hole cold extrusion[J]. Acta Aeronauticaet Astronautica Sinica, 2017,08:1-18
9. Elajrami M, Miloud R, Milouki H, et al. Experimental investigation of the effect of double cold expansion on the residual stress distribution and on the fatigue life of rivet hole[J]. Journal of the Brazilian Society of Mechanical Sciences & Engineering, 2015:1-6.
10. W.C. Liu, J. Dong, P. Zhang, A.M. Korsunsky, X. Song, W.J. Ding. Improvement of fatigue properties by shot peening for Mg-10Gd-3Y alloys under different conditions[J]. Materials Science & Engineering A. 2011(18):102-115.
11. S.M. H-Gangaraj, Y. Alvandi-Tabrizi, G.H. Farrahi, G.H. Majzoobi, H. Ghadbeigi.Finite element analysis of shot-peening effect on fretting fatigue parameters[J].Tribology International. 2010(11):56-67.
12. Pirri A N, Root R G, Wu P K S. Plasma Energy Transfer to Metal Surfaces Irradiated by Pulsed Lasers[J]. Aiaa Journal, 2012, -1(12):1296-1304.

13. Hu T, Qiao H, Zhao J, et al. Development of laser shock peening equipment[J]. Opto-Electronic Engineering, 2017, 44(7):732-737.
14. Duesler P W, Filewich P. Methods for testing laser shock peening[J]. 2017:56-70.
15. Filewich P. Sequencing of multi-pass laser shock peening applications[J]. 2017:35-48
16. Kalainathan S, Prabhakaran S. Recent development and future perspectives of low energy laser shock peening[J]. Optics & Laser Technology, 2016, 81:137-144.
17. Zhong Minlin, Liu Wenjin. Leading areas and hot topics on global laser materials processing research［J］. Chinese J. Lasers, 2008, 35(11): 1653～1659
18. P Peyre, L Berthe, X Scherpereel, et al. Experimental study of laser-driven shock waves in stainless steels[J]. Journal of Applied Physics, 1998, 84(11): 5985~5997.
19. P Peyre, L Berthe, R Fabbro, et al. Experimental determination by PVDF and EMV techniques of shock amplitudes induced by 0.6-3ns laser pulses in a confined regime with water[J]. Journal of Physics, 2000, 33(50): 498~503.
20. Y Sano, N Mukai, K Okazaki, et al. Residual stress improvement in metal surface by underwater laser irradiation[J]. Nuclear Instruments and Methods in Physics research Section, 1997, 121(1~4): 432~436.
21. M Morales, J A Porro, M Blasco, et al. Numerical simulation of plasma dynamics in laser shock processing experiments[J]. Applied Surface Science, 2009, 255: 5181~5185.
22. S Montross Charles, W Tao, et al. Laser shock processing and its effects on microstructure and properties of metal alloys: a review[J]. International Journal of Fatigue, 2002, 24: 1021~1036.
23. A S Brown. A shocking way to strengthen metal[R]. In: Aerospace America, 1998. p. 21~24.
24. S Mannava, A E McDaniel, W D Cowie. US Patent 5,492,447[R]. General Electric Company, 1996.
25. Universal Technology Corporation. High Cycle Fatigue(HCF) Science and Technology Program 1999 Annual Report[R]. 2000
26. B Cowles, B Morris, R Naik, et al. Applications, benefits, and challenges of advanced surface treatments-An industry perspective[C]. Presented at the First International Conference on Laser Peening, 2008.

27. Lu Jinzhong. Mechanical properties and microplastic deformation mechanism of aluminum alloy strengthened by laser shock [D]. Jiangsu University, 2010.
28. C O Lykins, Laser shock peening vs. Shot peening: A damage tolerance investigation, proceedings surface treatment of titanium alloys[R]. Cincinnati OH,1996
29. D W Sokol, A H Clauer. Applications of laser peening to titanium alloys[C]. Presented at the ASME/JSME 2004 Pressure Vessels and Piping Division Conference. San Diego: CA, July 25~29, 2004
30. R H Michael, T D Adrian, G D Anne, et al. Laser peening technology[J]. Advanced Materials & Processes, 2003, 161(8): 65~71.
31. M J Leap, J Rankin, J Harrison, et al. Effect of laser peening on fatigue life in an arrestment hook shank application for naval aircraft[C]
32. Lawrence Livermore National Laboratory. Science & Technology Review[R]. America, 2001.
33. Lawrence Livermore National Laboratory. Program Update[R]. America, 2003
34. Braisted W, Brockman R. Finite element simulation of laser shock peening [J]. International Journal of Fatigue, 1999,21(7): 719-724.
35. Cao Jinfeng, Shi Yiping. ABAQUS Finite Element Analysis FAQ. Beijing: China Machine Press, 2009.
36. Wang Bohan, Chen Li, Ding Junliang, et al. Numerical Simulation of TC4 Titanium Alloy [J]. Journal of Aerospace Power. 2021, 36(5):959-968.
37. Ding K, Ye L. Laser shock peening performance and process simulation[M]. New York: Woodhead, 2006.